From INSTITUTE OF ENVIRONMENTAL MEDICINE
Karolinska Institutet, Stockholm, Sweden

ENGINEERED CORE – SHELL NANOPARTICLES: SYNTHESIS, CHARACTERIZATION AND BIOCOMPATIBILITY STUDIES

Carmen Mihaela Vogt

Karolinska Institutet

Stockholm 2012

Cover: Core – shell nanoparticles – protein corona internalised by human primary macrophages
Published by Karolinska Institutet. Printed by Universitetservice US-AB

ISBN 978-91-7457-789-1

ABSTRACT

Superparamagnetic iron oxide nanoparticles (SPIONs) have emerged as promising contrast agents for Magnetic Resonance Imaging (MRI). Some SPIONs are already approved for clinical use. Coating of these nanoparticles with an additional biocompatible layer serves to improve the colloidal stability and biocompatibility. The present thesis is focused on the synthesis, characterization, and in vitro biocompatibility assessment of SPIONs as well as the assessment of the potential impact of the so-called bio-corona on the surface of these nanoparticles on their behavior. In addition, synthesis and magnetic evaluation of novel nanocomposites was also performed.

In Paper I, the production of mono-dispersed, necking-free, single-core iron oxide-silica shell nanoparticles with tunable shell thickness was achieved by a carefully optimized inverse microemulsion method. The development of novel nanomaterials for biomedical applications need to be accompanied by careful scrutiny of their biocompatibility with a particular focus on the possible interactions with the primary defense system against foreign invasion, the immune system. Consequently, in Paper II, our efforts in synthesizing high quality core–shell nanoparticles with superparamagnetic character and sufficiently high magnetization were coupled with in vitro biocompatibility assessment and studies of cellular internalization using primary human macrophages and dendritic cells. The silica-coated nanoparticles were nontoxic to primary human monocyte-derived macrophages at all doses tested whereas dose- and size-dependent toxicity was observed for primary monocyte-derived dendritic cells exposed to smaller silica-coated nanoparticles, but not for the same-sized, commercially available dextran-coated iron oxide nanoparticles. Furthermore, the silica-coated iron oxide nanoparticles were taken up in both cell types through an active, actin cytoskeleton-dependent process to a significantly higher degree when compared to the dextran-coated nanoparticles, irrespective of size. This has potentially useful implications for labeling of immune cells for visualization, diagnosis or treatment of inflammatory processes.

When nanomaterials confront physiological media, the formation of a "corona" of proteins by adsorption to the surface of nanomaterials occurs which will influence how the particles will interact with a biological system and consequently will affect the fate of the particles. The potential effect of the protein corona on the magnetic and biological behavior of silica- versus dextran-coated SPIONs was addressed in Paper III. A thorough physical characterization of SPIONs without and with a protein corona as well as in vitro biocompatibility and cellular internalization using human primary macrophages was performed. Modulation of the magnetization and relaxivity signals of the SPIONs was noted following interaction with human plasma proteins. Macrophage viability was influenced by the presence or absence of a protein corona on silica-coated SPIONs but in the case of the dextran-coated SPIONs. Macrophage production of pro-inflammatory TNF-α was not triggered by SPIONs with or without a corona. Moreover, comprehensive assessment of the protein corona using mass spectrometry and bioinformatics tools revealed distinctive compositions on the two types of nanoparticles. Further studies need to be performed to understand the interrelationship between the acquired protein corona on the SPIONs and their function as MRI contrast agents.

In Paper IV, incorporation of iron oxide nanoparticles homogeneously dispersed in a polymeric matrix and assessment of the magnetic and optical properties of the resulting structured nanomaterials are presented. Magnetic evaluation of the nanocomposite revealed its ferromagnetic properties while the low loading of nanoparticles with very good distribution in the nanostructure yielded materials with good magneto-optical properties. These materials have potential applications as micro actuators, sensors, relays and magneto optical devices based on the Faraday effect.

Overall, this thesis attempts an interdisciplinary approach to the synthesis and characterization of nanomaterials and their biocompatibility assessment, with the aim to enable future applications in nanomedicine.

LIST OF PUBLICATIONS

This thesis is based on the following papers which will be reserved by their Roman numbers:

I. CARMEN VOGT, Muhammet S. Toprak, Sophie Laurent, Jean-Luc Bridot, Robert N. Müller, Mamoun Muhammed, High quality and tuneable silica shell - magnetic core nanoparticles, Journal of Nanoparticle Research, 2010, 12, 1137-1147

II. Andrea Kunzmann*, Britta Andersson*, CARMEN VOGT, Neus Feliu, Fei Ye, Susanne Gabrielsson, Muhammet S. Toprak, Tina Buerki-Thurnherr, Sophie Laurent, Marie Vahter, Harald Krug, Mamoun Muhammed, Annika Scheynius, Bengt Fadeel, Efficient internalization of silica-coated iron oxide nanoparticles of different sizes by primary human macrophages and dendritic cells, Toxicology and Applied Pharmacology, 2011, 253, 81–93

III. CARMEN VOGT, Maria Pernemalm, Pekka Kohonen, Roland Grafström, Sophie Laurent, Janne Lehtiö, Muhammet Toprak, Bengt Fadeel, Comprehensive analysis of the corona of plasma proteins on superparamagnetic iron oxide nanoparticles with different surface coatings, *(manuscript)*

IV. Andrea Fornara, CARMEN VOGT, Najmah Najmoddin, Sergiy Khartsev, Shanghua Li, Jian Qin, Muhammet S. Toprak, Alexander Grishin, Mamoun Muhammed, Synthesis, structural and magnetic characterization of transparent magnetic iron – oxide/PMMA nanocomposite, *(manuscript)*

*These authors contributed equally to this publication

TABLE OF CONTENTS

LIST OF ABBREVIATIONS

TEM	Transmission Electron Microscope
SEM	Scanning Electron microscope
STM	Scanning Tunneling Microscope
AFM	Atomic Force Microscopy
CT	Computed Tomography
MRI	Magnetic Resonance Imaging
MPIO	Micrometer sized paramagnetic iron oxide
SPIO	Superparamagnetic iron oxide
USPIO	Ultrasmall superparamagnetic iron oxide
SPION	Superparamagnetic iron oxide nanoparticles
RES	Reticular endothelial system
PVA	Polyvinyl alcohol
$Fe(acac)_3$	Iron(III) acetylacetonate
TEOS	Tetraethyl orthosilicate
PMMA	Polymethyl methacrylate
PS	Polystyrene
MEMS	Microelectromechanical systems
PEG	Polyethylene glycol
CSNP	Core – shell nanoparticles
AAS	Atomic absorption spectroscopy
ICP	Inductively Coupled Plasma
FTIR	Fourier Transform Infrared Spectroscopy
ATR	Attenuated Total Reflectance
XRD	X-ray powder diffraction
DLS	Dynamic light scattering
TGA	Termogravimetric analysis
DSC	Differential scanning calorimetry
UV – VIS	Ultraviolet – visible spectroscopy
VSM	Vibrating sample magnetometer
AGM	Alternating gradient magnetometer
FR	Faraday rotation
CD14	Cluster of differentiation 14
DC	Dendritic cells
APCs	Antigen-presenting cells
GM-CSF	Granulocyte-macrophage colony-stimulating factor
CD1a	Cluster of Differentiation 1a
CD11c	Complement component 3 receptor 4 subunit
CD83	Cluster of Differentiation 83
PBMC	Peripheral blood mononuclear cell
M-CSF	Macrophage colony-stimulating factor
EMR1	Human epidermal growth factor module-containing mucin-like receptor 1
LAL	Limulus Amebocyte Lysate
LPS	Lipopolysaccharide
MTT	3-(4,5-dimethythiazol-2-yl)-2,5-diphenyl tetrazolium bromide
PI	Propidium Iodide
PS	Phosphatidylserine
FACS	Flow cytometry Fluorescence-activated cell sorting
ELISA	Enzyme-linked immunosorbent assay
MS	Mass spectrometry
ICP-MS	Inductively coupled plasma mass spectrometry
SOM	Self Organizing Maps
PAM	Partitioning around medoids
GO	Gene Ontology
MF	Molecular function
BP	Biological process

CC	Cellular component
KEGG	Kyoto Encyclopedia of Genes and Genomes
HRTEM	High Resolution Transmission Electron Microscopy
FCS	Fetal calf serum

1 INTRODUCTION

Nanostructured materials and more specifically nanoparticles have been a permanent encounter in everyday life of humans throughout the humankind history (1). The relationship started with the first tools fabrication were the particles and most probably, nanoparticles were accidentally inhaled. The discovery of fire, apart from a fantastic dietary improvement and other advantages, also brought along accidental inhalation of carbon nanoparticles produced by burning wood. The artists of the prehistoric age were exposed to iron oxide, manganese dioxide, charcoal, kaolin or mica nanoparticles in the attrition process of producing their pigments. Much later, the ancient Egyptians were exposed to lead nanoparticles from the make-up products. Silicosis affecting miners and stone workers, described already by ancient Greeks and Romans, is today known as an effect of long exposure to silica micro and nanoparticles.

The 20th century, especially after the Second World War, associated with an extraordinary development of techniques that could visualize small entities: Transmission Electron Microscope (TEM) – 1931, Scanning Electron Microscope (SEM) – 1935, Scanning Tunneling Microscope (STM) – 1985 and Atomic Force Microscope (AFM) - 1986. In addition, it brought an explosion of scientific interest in making smaller and smaller engineered features from bulk materials driven by the incentive of improving different areas of life as medicine, computer science, and energy storage. This correlated with a higher (and increasing) exposure of humans to nanoparticles to an unprecedented level in history either accidentally (environmental pollution, accidental work exposure) or through various products that contain nanoparticles: cosmetic products, clothes, medicines etc (2).

This thesis is attempting an integral approach containing aspects related to synthesis of engineered nanoparticles and their biomedical applications as well as reflecting on to the impact of nanomaterials in biological systems. Understanding biological, toxicological effects of nanoparticles is crucial for the safe and sustainable development of nanomedicine (3).

1.1 NANOSTRUCTURED MATERIALS

The term nano (from Greek nano meaning dwarf) is used for designating very small features, nano representing 10^{-9}m.

Often superimposed, the terms of nanostructures and nanostructured materials are complementary. Nanostructures are defined as entities characterized by form and at least one dimensionality in nanoscale range, while nanostructured materials are not only composed of building units having nanoscale dimensions but they are characterized additionally by composition (4, 5). In Table 1 are enumerated examples of the elementary building units of nanostructures. For the complete classification of the nanostructures that include 36 classes see the reference (5).

Table 1. Elementary building units of nanostructures

0D	Fullerenes, nanorings, nanoparticles, core – shell nanoparticles, nanopowders, clusters
1D	Nanorods, fibers, filaments, nanotubes, spirals, nanowires, ribbons
2D	Nanofilms, nanomembranes

The structures enumerated above are associated to sizes less the 100 nm that induces new physicochemical properties compared to the conventional formulations of the materials. The novel properties observed are attributed to their (i) morphology described by size induced effects (large surface area, narrow size distribution) and shape (spherical versus rod); (ii) controlled chemical composition: high purity, controlled crystallinity etc; (iii) surface structure: increased surface reactivity, inorganic or organic surface coatings; (iv) solubility and (v) aggregation versus colloidal stability.

Figure 1 represents the inverse relationship between the particles size and the number of the molecules (or atoms) on the surface of a spherical nanoparticle. For sizes under 100 nm the number of surface molecules increases exponentially with the decrease of the diameter. For a particle of 3 nm approximately 80% of its atoms/molecules are on the surface whereas for a nanoparticles of 30 nm diameter <10% of its constituents molecules are on the surface (2).

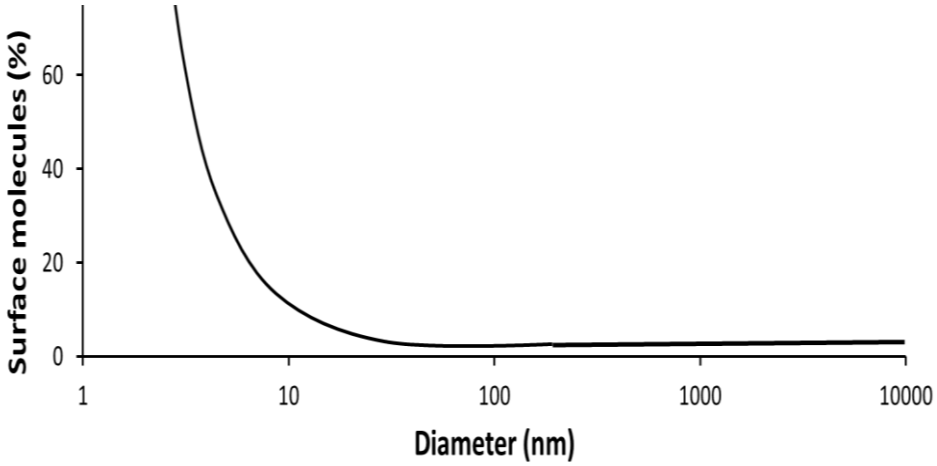

Figure 1. The diameter – surface molecules relationship for spherical particles (2)

The same properties that lead to novel applications of nanomaterials in high end area as biomedical application, energy storing devices, computer industry might lead additionally to unique (potentially hazardous) effects in biological systems (6, 7). In the next sections, we will review the specific applications of magnetic nanoparticles and magnetic nanocomposites related to the particular characteristics of magnetic nanoparticles. Additionally the safety assessment of possible exposure to nanoparticles is discussed and their possible toxicity associated to the interactions they might have with the biological environments.

1.2 MAGNETIC NANOPARTICLES

Two major magnetic iron oxide phases are used in medical applications: magnetite (Fe_3O_4) and maghemite (γ -Fe_2O_3). The preparation methods are critical in determining their properties: particle size and size distribution, shape, surface properties, magnetic properties, which are consequently influential on their applications (8).

Iron oxide nanoparticles synthesis

Numerous methods can be applied to synthesize magnetic iron oxide nanoparticles. The most commonly used methods are: co-precipitation, sol-gel synthesis, microemulsion synthesis, hydrothermal reactions, polyol method, thermal decomposition of precursors apart from less common techniques as spray and laser pyrolysis (9-11), electrochemical methods (12, 13) and flow injection synthesis (14).

The co-precipitation method is probably the simplest one allowing the preparation of large quantities of nanoparticles in one batch. The iron oxides are prepared by mixing

ferrous and ferric salts in aqueous media (non oxidizing environment) at high pH (15, 16). The properties of precipitated iron oxides (incl. size, shape, composition) depend on the type of salts used as precursors (nitrates, sulfates, chlorides), molar ratio of the starting precursors, reaction temperature, pH and ionic strength of the media (17). Significant control on the size of the resulting particles can be achieved if during the formation of iron oxide nanoparticles chelating organic anions (carboxylate ions: citric, gluconic, oleic acid), or polymers as: polyvinyl alcohol (PVA), dextran, starch are added (18).

Another method used for the synthesis of iron oxide nanoparticles is sol-gel technique. Sol-gel methods generally refer to the hydrolysis and condensation of metal alkoxides precursors that result in a colloid/"sol" of oxide nanoparticles. The ''sol'', by further condensation and polymerisation leads to a three dimensional network called "gel" containing the liquid phase (19). By subjecting the gels to elevated temperatures the nanoparticles acquire the final crystalline state. The properties of the gel are influenced by the solvent used, temperature, type of precursors utilized, pH and hydrodynamic conditions (8). This method is also suitable for production of large quantities of iron oxide nanoparticles.

Water-in-oil microemulsions, called also inverse microemulsions, are alternatively used to obtain iron oxide nanoparticles with narrow size distribution and controlled morphology. The nanosized droplets of water dispersed in the oil phase and stabilized by surfactant molecules (at the oil/water interface) are confined environments limiting the growth in the formation process of the nanoparticles (20). Varying the size of the aqueous pool phase (or the ratio between the organic and water phase) is the main factor regulating the water droplet size and the iron oxide phase size. Other factors as reaction temperature, concentration of the reactants, flexibility of the surfactant film may also influence the final particles size (21-23).

Another route used for synthesizing iron oxide nanoparticles is the hydrothermal method. This method is simple, versatile and environmentally friendly route with no organic solvent involved and no post reaction treatment as calcination being necessary (24). The reactions are carried out in aqueous media at high pressures (>2000 psi) and elevated temperatures (200-300 °C). The solvent content, temperature and time (25)

have important influence on the resulting nanoparticles by influencing the nucleation and growth processes.

The polyol method is a facile method of synthesizing nanoparticles with well-defined size and shape, narrow size distribution compared with the aqueous route (26). The solvents (ex. ethylene glycol, diethylene glycol, polyethylene glycol) dissolve the inorganic precursors, but due to their high boiling point. Moreover they act as reducing agents and as stabilizing agents preventing the aggregation of newly formed particles (27). The obtained nanoparticles are easily dispersible in polar solvents being coated with a hydrophilic ligand.

A high degree of monodispersity and a greater control on the size of the nanoparticles can be achieved using synthesis methods as high temperature decomposition of metallo-organic iron precursors. Iron oxide particles with well control on the size ranging from 4 to 20 nm (28-30) are obtained from the thermal decomposition of $Fe(Cup)_3$, $Fe(CO)_5$, $Fe(acac)_3$ in the presence of surfactants. Using iron chloride salts or other iron oxides as precursors is a much more environmental friendly alternative and is becoming an increasingly used method for obtaining easily tunable size iron oxide nanoparticles (31-34). The nanoparticles obtained are well-separated, dispersible in organic solvent, various treatments being necessary to make these particles dispersible in water.

Core shell nanoparticles synthesis.

The core-shell nanoparticles are excellent candidates for increasing the intrinsic functionalities and building up progressively more complicated structures.

The magnetic core can be used for targeting by an external field. In addition, it allows localization and visualization through MRI of the effects of the active substance incorporated in/adsorbed on the surface of the shell. Additionally, the magnetic core can be used as an alternative treatment modality via hyperthermia therapy.

Silica offers an inert coating material on the magnetic core that inhibits their aggregation in liquid media, enhances their chemical stability and offers a versatile platform for surface modification. Furthermore, dye incorporation or quantum dots

inclusion into the shell adds an extra function of detection and localization under excitation using different wavelength of radiation.

Silica coating methods.

Silica is one of the most researched materials for coating magnetic and metallic nanoparticles. It increases the chemical stability and biocompatibility of the core particles as well as their colloidal stability by isolating the magnetic dipoles through the silica shell and inducing electrostatic repulsion (silica is negatively charged at physiological pH).

For the formation of silica shell on the cores, two main approaches are followed, both of them originally used for producing silica nanoparticles. In the first method, known as Stöber process (35), silica is formed on the surface of the iron oxide cores by hydrolysis and condensation of a precursor as tetraethyl orthosilicate (TEOS). In basic media TEOS undergoes hydrolysis and polycondensation reactions that results in formation of amorphous silica. The method is very versatile, the adjustment of the silica shell being possible by varying several parameters: the solvent type (higher molecular weights alcohols form larger core- shell nanoparticles), the concentration of iron oxide nanoparticles (lower concentrations of iron oxide conduct to bigger composites nanoparticles), the concentration of the silica precursor, the concentration of ammonia catalyst and the water (36-39).

The synthesis of uniform silica shells, with single core and controlled thickness is still a challenge, although the method is relatively simple and a lot of research was and is still conducted on core-shell nanoparticles with silica shell. The microemulsion method is an alternative to Stöber technique (40, 41). Water-in-oil microemulsion (w/o) or inverse microemulsion was extensively studied and used for the production of silica nanoparticles with a narrow size distribution (42-47). This route is becoming favored for the synthesis of core –shell nanoparticles, the inverse micelles being used as a confinement and controlling factor for the growth of the silica shell (48-52).

Due to the condensation reactions that continue during the post synthesis processing, the particles produced are strongly necked and aggregated, even though the method has the advantage of greatly controlling the thickness of the silica shell. The aggregation

and necking result in an increase of the overall size of the particles, decrease in the surface area and reduced stability of the particles in colloids.

This thesis is specifically addressing solving the aggregation issue of the particles obtained by inverse microemulsion method (Paper I). Well-dispersed, perfectly separated (without the presence of interparticle bridging) and single core-shell nanoparticles with an excellent control of the shell thickness are obtained and are shown to be biocompatible (Paper II).

Specific magnetic properties

The magnetic nanoparticles and the structures in which the magnetic nanoparticles are incorporated have to undergo complex magnetic characterizations in order to assess their magnetic properties and the potential applicability in medical areas where these features are essential (i.e. MRI).

When the magnetic properties of a material are assessed, the value of magnetic moment for the sample is a sum of the magnetic moments of the atoms from the sample. This value is influenced by several parameters, some sample dependents: the size of the sample and the magnitude of the magnetic ordering, other measurement conditions dependent as temperature and applied magnetic field.

The iron atom, due to its four unpaired electrons in 3d orbitals, has a high magnetic moment. When iron atoms form crystals, different magnetic behaviors can occur (figure 2).

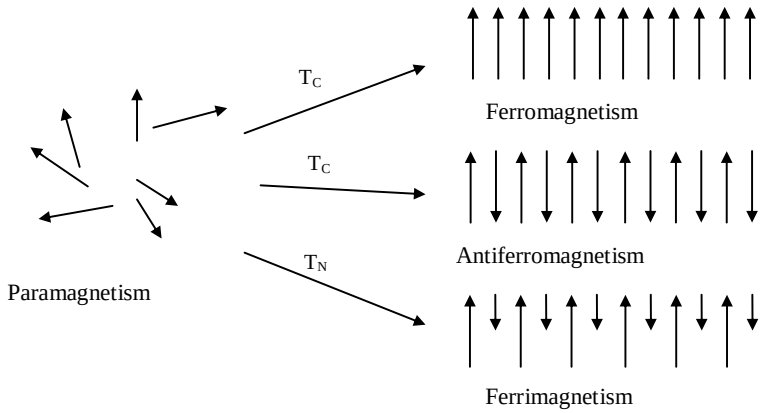

Figure 2. Alignment of individual atomic magnetic moments in different types of materials. (53)

In the materials with a paramagnetic behavior, the magnetic moments of the atoms are randomly aligned, the crystal having a zero net magnetic moment. If this crystal is under an external magnetic field, the crystal will have a small net magnetic moment due to the alignments of some of the moments. A ferromagnetic crystal has all the moments aligned even in the absence of a magnetic field. In a ferrimagnetic crystal, the net magnetization is the sum of individual atomic magnetic moments that are arranged antiparallel and that have different strength. If the antiparallel moments are equal in magnitude, the crystal is antiferromagnetic and the net magnetic moment is zero.

The ordered arrangement of the magnetic moments decreases with the increase in the temperature (due to thermal fluctuations of the magnetic moments of the atoms). For ferro-, ferri- and antiferromagnetic materials is defined a critical temperature below which a spontaneous magnetization is present: Currie temperature (*T*c) for ferro- and ferrimagnetic materials and Néel temperature (T_N) for antiferromagnetic materials.

Large particles and bulk materials have a multidomain structure, with regions of uniform magnetization being separated by domain walls (fig 3).

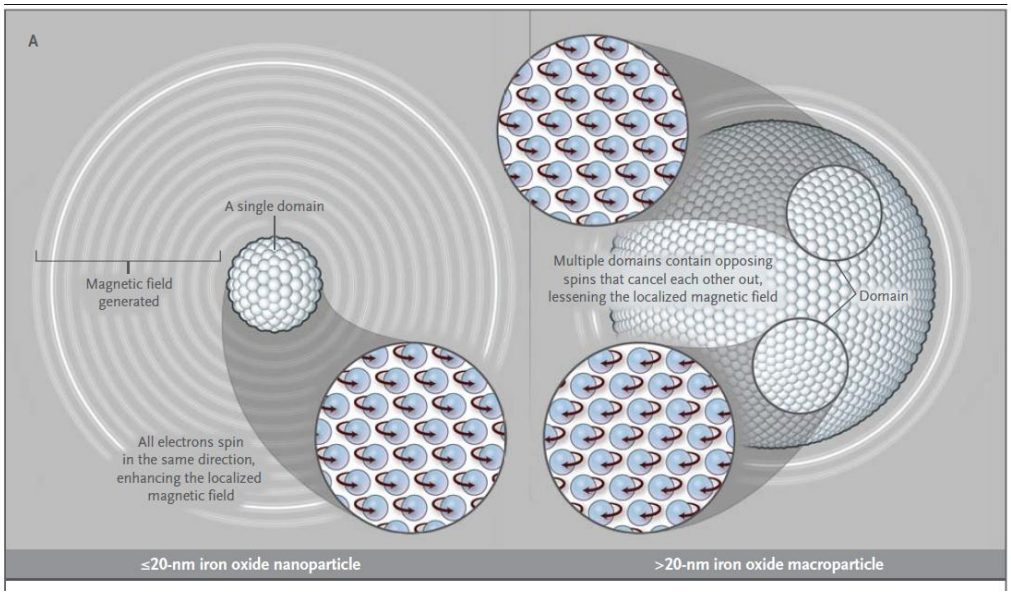

Figure 3. Single domain nanoparticles versus multidomain structure of a bulk magnetic material (54)

When the particle size of the material decreases the number of the domains decreases until it reaches one single domain (below a critical size D_C, material dependent). A

single domain particle uniformly magnetized has all the spins aligned in the same direction that results in very high coercivity (18).

When a ferromagnetic material of magnetization *M* is subjected to a magnetic field *H*, a magnetization curve with a hysteresis is obtained (Figure 4 (a)). *M* increases under an increasing *H* till it reaches a maximum value called saturation magnetization M_s. When *H* decreases, the domains do not return to their original orientation, the material having a residual magnetization called remnant magnetization M_R which can be annulated by applying a magnetic field in the opposite direction of the initial field, H_C.

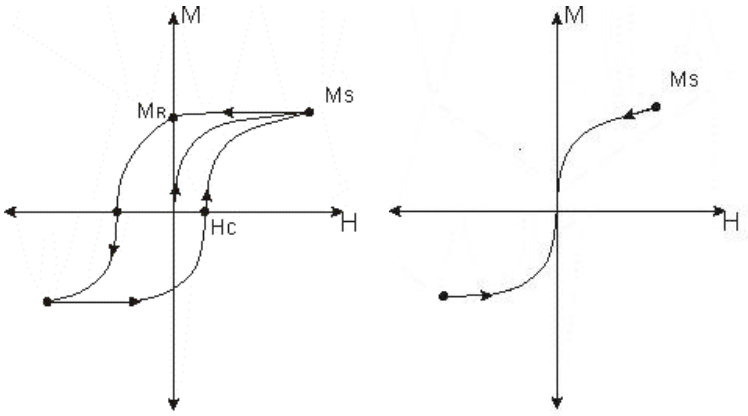

Figure 4. Magnetization hysteresis curves of (a) ferromagnetic and (b) superparamagnetic materials.

Another important parameter that characterizes the monodomain particles is the anisotropy energy. It represents the preference of the magnetization to orient along preferential directions in the nanoparticles (relative to the crystallographic directions). The axes along which the magnetic energy is minim called easy axes or anisotropy directions.

The anisotropy energy is a function of the tilt angle: $E = K_{eff} V \sin^2 \theta$ (1)

K_{eff} is the effective uniaxial magnetocrystaline anisotropy constant, *V* is the volume of the particles and θ is the angle between the magnetization direction and the easy axis. The anisotropy energy is dependent on several factors as shape of the crystal, bulk magneto crystalline anisotropy and the agglomeration degree that give rise to dipole interaction between neighboring particles.

For single monodomain particles, the anisotropy energy is comparable with the thermal energy: $E_T = k_B T$ (2)

k_B is Boltzmann constant and T is the absolute temperature.

When $k_B T << K_{eff} V$, the magnetic moment is fixed along the easy axis of the magnetisation, thermal energy being too small to overcome the anisotropy barrier. The nanoparticles are called then thermally blocked particles with the magnetic moment "blocked" along a specific easy axis (crystallographic direction).

When $k_B T >> K_{eff} V$ the system behaves paramagnetic with the magnetic moments randomly arranged, the thermal energy being high enough to deviate the magnetic moment from the easy axis. The atoms are ferromagnetically coupled resulting a "super" moment inside of each particle, phenomenon called superparamagnetism (55).

In a magnetic field the superparamagnetic nanoparticles have no remanent magnetisation, no coercivity while maintaining a very high saturation magnetization (8) (figure 4(b)).

Characteristic of superparamagnetic nanoparticles is Néel relaxation time, τ_N, the time necessary for magnetisation to return to equilibrium after perturbation:

$$\tau_N = \tau_0 e^{\frac{KV}{k_B T}} \quad (3)$$

where τ_0 is the characteristic relaxation time (anisotropy energy dependent), k_B Boltzmann constant, T the absolute temperature.

The equation 3 shows that the Néel relaxation time is dependent on the nanoparticle volume and the temperature.

1.3 MAGNETIC NANOCOMPOSITES

Magnetic nanocomposites are 3D nanostructured materials with 0D structures (magnetic nanoparticles) dispersed in a polymeric matrix. They combine the properties of the polymeric matrix: lightweight, versatile processing, various mechanical properties with the properties of the dispersed inorganic nanoparticles: superparamagnetism, ferromagnetism, electron and photon transport, size dependent band – gap. Thus, novel materials with advanced new functions and applications can be obtained (56). A critical challenge in synthesizing a nanocomposite material is to

achieve a uniform dispersion of the nanoparticles in the polymer matrix with minimal clustering. The clustering of the inorganic fillers is influenced by particle–particle and particle–matrix interactions. It is therefore important to design synthetic and processing strategies of the polymeric nanocomposites in which the internal steric forces are overcome, and the nanoparticles are prevented from forming larger agglomerates. The in situ polymerization and in situ formation of the nanoparticles are chemical methods that are an alternative to the physical methods of mixing particles in the polymeric melts successfully obtaining transparent nanocomposites (56).

For applications where magnetic properties are desired, using nanoparticles with magnetic properties is necessary. Metals such as Fe (57), metal alloys as CoPt (58), oxides as ferric oxides (59) and ferrites (60) are used as inorganic fillers. The polymeric matrix material is chosen depending on the intended application as vinyl esters (61) where high mechanical and chemical resistance is required like in car industry, or polymethyl methacrylate (PMMA), polystyrene (PS) where transparency is needed like in microelectromechanical systems (MEMS): micro actuators, sensors, relays and magneto-optical devices based on the Faraday effect (62). Paper IV deals with synthesis of magnetic nanocomposites.

1.4 BIOMEDICAL APPLICATIONS OF NANOMATERIALS

Nanomedicine, which sees in the latest years an extensive research effort and development, represents the application of nanotechnology in medicine. Drug delivery and diagnostics/imaging are the main areas in medicine where nanomaterials find applications.

Diagnostic applications. The imaging techniques are used in clinics to detect diseases at an early stage, to monitor the effect of therapeutics as well to monitor the evolution of the disease during the medical treatment and post therapy phase.

In imaging, contrast refers to the signal differences between adjacent regions and is an important parameter that is used for differentiating between different type of tissues and between healthy and disease affected tissue. While the contrasting effect X-ray and computer tomography (CT) is a direct contrast due to the electron density difference in Magnetic Resonance Imaging (MRI), the contrast enhancement is an indirect contrast

resulting from the interaction between the contrast agent and the neighboring water protons.

MRI, among other non-invasive imaging techniques such as computed tomography (CT), positron emission tomography (PET), ultrasound (US) and optical imaging (OI), is one of the most used methods in research as well as in clinics due to its capability of imaging the soft tissue structures (40). Primarily used for producing anatomical images, MRI gives also information on the physiochemistry of the tissue, flow, diffusion and motion (63).

The fundamental principle of MRI is that unpaired nuclear spins (mainly from hydrogen atoms in water: 70% to 90% of most tissues and organic compounds) align themselves when exposed to a magnetic field. A temporary radiofrequency pulse change the alignment of the spins, and their return to baseline (relaxation) is recorded as a modification in electromagnetic flux. Protons from different tissues react differently giving a picture of anatomical structures (64). Two independent processes, longitudinal (or spin-lattice) relaxation (T1-recovery)(fig. 5a) and transverse (or spin-spin) relaxation (T2-decay)(fig. 5b), can be monitored to generate an MR image.

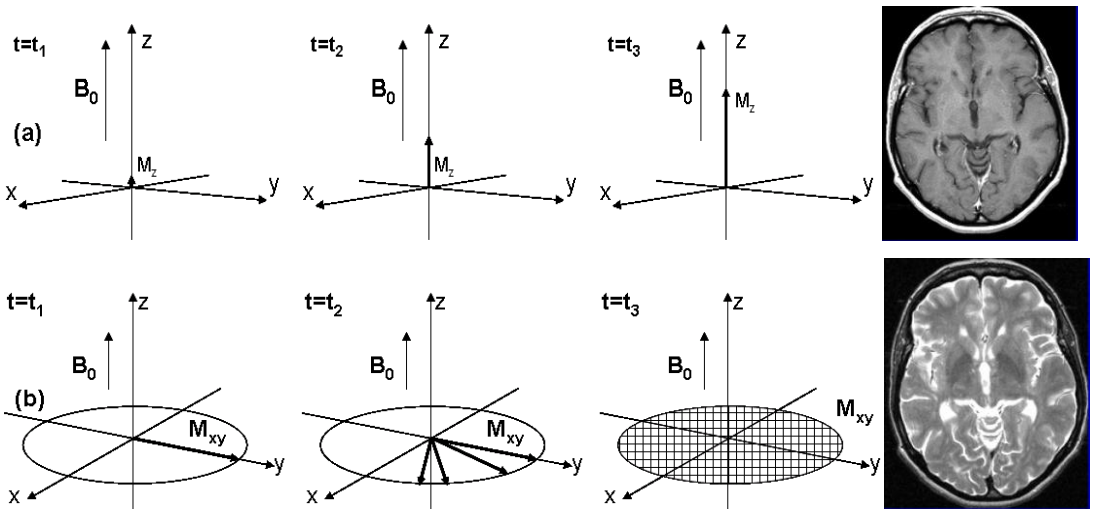

Figure 5. T1 recovery(a) and T2 decay(b)(65)

MR imaging is considered to be highly sensitive (to show pathological changes in a tissue) but not so specific (i.e. different pathologies have similar appearances) (65). The development of chemically synthesized contrast agents has helped MRI become a

powerful tool for clinical diagnosis and biomedical research (66). Contrast agents help to improve the specificity by inducing a change in the behavior of the surrounding tissue (affecting the behavior of protons in their proximity), better tissue characterization and a reduction in image artifacts (67, 68). They enhance the image contrast between normal and diseased tissue and indicate the status of organ function or blood flow after administration by increasing the relaxation rates of water protons in tissue in which the agent accumulates (69).

Apart from general requirements as: tolerance, safety, toxicity, stability, osmolality, biodistribution, elimination and metabolism (68), contrast agents have to possess specific prerequisites as adequate relaxivity and susceptibility.

Currently available MRI contrast agents can be categorized into two broad groups: T_1-agents and T_2-agents. T_1-agents generally increase the longitudinal (or spin-lattice) relaxation rates ($1/T_1$) of water protons in tissue more than the transverse (or spin-spin) relaxation rates ($1/T_2$).

Soluble paramagnetic agents as gadolinium and manganese chelates are having dominantly T_1-lowering effect with an increase in signal intensity on T_1 weighted images (positive contrast agents). Nanoparticles that can carry a large number of paramagnetic T1 contrast molecules will produce a strong T1 contrast signal. Platforms as silica (70) and nanotubes (71) have been successfully used but they have sizes over 100 nm and low blood half time circulation. MnO nanoparticles are in the development stage as new T1-MRI contrast agents for brain, liver and kidney imaging (72).

The superparamagnetic iron oxide nanoparticles (SPION) are T_2-agents increasing the $1/T_2$ of tissue selectively leading to decreases in signal intensity on T_2 weighted images (negative contrast agents). The ability of SPIONs to perform as MR imaging contrast agents is actively investigated in the last 20 years (73). They are classified based on their size, which is affecting the biological distribution, as follows: (i) micrometer sized paramagnetic iron oxide (MPIO), ii) superparamagnetic iron oxide (SPIO) and iii) ultrasmall superparamagnetic iron oxide (USPIO). Commercial SPION as Ferridex®, Combidex®, Resovist®, AMI-228/Ferumoxytrol®) are dextran or other carbohydrate coated or citrate-stabilized particles (VSOP-C184) (74, 75) but SPION with other

coating materials (polymers, metals (gold, silver), silica) are either in the development phase or in different phases of the preclinical study.

When MRI contrast agents are coupled with molecular probes that recognize certain tissue signatures, then the visualization has an enhanced specificity to certain modification in the targeted tissue (73). Multifunctional nanoparticles find application in diagnosing some of the most prevalent diseases in humanity.

The multimodal specific imaging of cardiovascular diseases is one of the important impact applications. Multifunctional magnetic nanoparticles are proposed as MRI contrast agents for several clinical cardiovascular applications as myocardial injuries, and atherosclerosis. The increased uptake of SPION by the macrophages (hallmark cells in atherogenesis) and further functionalization of SPION with adhesion molecule (V-CAM) – target for endothelial and macrophage cells– will improve the early diagnosis and decrease the morbidity and mortality associated with atherosclerosis (73, 74).

Cancer imaging is another extremely important application of multifunctional magnetic nanoparticles as this disease is the second worldwide death cause. The early detection of the disease associated with early treatment increase the curability chances with dramatic social and economic impact. The current resolution limit of 2-3 mm (for liver tumors) and lymph metastases of 5-10 mm can be decreased significantly by active targeting (antigen – antibody reaction) of a specific marker expressed on the tumor cells or SPION labeling with a precursor lesions specific antigen (74). The drug loading of the targeted nanoparticles adds to the sensitive MRI agent particles the function of controlled drug carrier. Covalently bonded methotrexate on the magnetic nanoparticles and pH induced release of the antitumoral agent into the specific tumoral cells allowed MRI localizing the nanoparticles before and after the drug release (76).

If a cell can be sufficiently loaded with magnetic nanoparticles, cell tracking by MRI is another possible application with the resolution near to the size of the cell. Localizing pre-loaded cells with functionalized magnetic nanoparticles after transplantation or transfusion, apoptosis detection or monitoring enzymatic activities are just few of the new highly specialized multimodal MRI applications in medicine(8, 73).

Drug delivery. Most of the drugs in use today in medical treatments need periodical, frequent administration in order to obtain a long-term effect. Drug targeting/delivering by nanoparticles or nanocapsules reduces dosage and minimizes side effects, ensures the pharmaceutical effects, protects drugs against degradation and enhances drug stability. Many types of drug delivery nanosystems have been developed based on biocompatible materials as polymer nanoparticles (77-79), lipid-based nanoparticles (80-82), inorganic materials-based nanoparticles (83-85) and nanogels (86-88). More advanced systems can either respond to some physiological changes in the body (pH, temperature) – self regulated systems - or the drug release can be enhanced ad necesitum by an exterior triggering system (magnetic field or ultrasounds) (89-91). Nanoparticles that combine multiple imaging capabilities with delivering an active substance are the next generation "theranostic". Magnetic nanoparticles are obvious candidates for designing theranostic agents. Using dextran coated SPIONs of 10 nm loaded with Alexa Fluor 750 and a potent photosensitizer (92) enhanced photodynamic therapy properties can be achieved. Gold-coated iron oxide nanoparticles can be used for combined molecular specific MRI/optical imaging and photothermal therapy of cancer cells (93).

1.5 SAFETY ASSESSMENT OF NANOMATERIALS

Safety assessment is an interdisciplinary approach that is trying to understand and measure the hazard and the exposure to a certain factor with the goal of assessing the risk associated with it.

Factors that must be addressed in assessing a risk associated with a substance or nanoparticles include dose, exposure routes, and biokinetics. Especially when performing safety assessment for nanoparticles a thorough physical chemical characterization is important as the nanoparticles characteristic is tightly associated with their effects (94).

1.5.1 Nanotoxicology – Overview

Toxicology is the study of the adverse effects of physical or chemical agents on living organisms. The principle that the risk posed by a substance is proportional to the potential to cause a hazard and with the amount of substance that the biological system is exposed to is one of the basic principles in toxicology(95). Nanotoxicology that is the study of the effect of nanoparticles on living organisms (96). This multidisciplinary

science integrates the understanding on the materials characteristics of the nanoparticles with its potential toxicity. Notably, exposure assessment is also needed for risk assessment of nanomaterials.

One characteristic of the nanostructure materials is their small size and the properties associated with it that might render them toxicity compared to the bulk form of the same material. In this light, it has to be emphasized that the toxicity is associated to a certain entity characterized by size, chemical composition, shape, surface charge etc. It is therefore essential to not discuss about nanoparticles in general terms but to identify them in the context of their possible biological interactions.

Dose. The toxicity of nanomaterials is strongly associated with the notion of dose and the way this is expressed i.e. mass versus particles number versus surface area. 1mg of 10 µm spherical carbon nanoparticles contains 10^{12} nanoparticles with a total surface area of 270 m^2 whereas 1mg of 10 nm of the same materials contains 10^{21} nanoparticles with a total surface area of 270 000 m^2 (97). At least two ways of expressing the dose allows a better understanding of the observed effects of nanoparticles (98). Furthermore, due to surface binding of molecules in biological media and eventual change in the agglomeration state of the nanomaterials, the effective surface area is another parameter that has to be considered in expressing the dose of a material (99).

Exposure route and biokinetics. The toxicity of nanoparticles to a biological system is highly dependent on which organ or cell types are exposed primarily. The toxicokinetics: uptake, transport, metabolism, accumulation in different organs and the final elimination of the nanoparticles from the organism is equally important when discussing about the nanotoxicity. There are various ways through which the nanoparticles are potentially encountering the biological systems: inhalation via the respiratory system, via dermic or mucosal membranes, enteral via gastrointestinal tract and parenteral via injection in different body tissues (1). The latter is certainly of great relevance in medicine.

For engineered nanomaterials (nanoparticles, nanofibers, nanotubes) that are formulated as powders, in a scenario of occupational exposure, lung is a primary organ for exposure. Exposure of rats to TiO_2 particles of various sizes (12 nm-250 nm) induced a size dependent acute inflammatory response followed by a remise of the

response to control levels 64 weeks post exposure. The smaller particles accumulated within the lung longer time than the bigger particles that were translocated in the interstitium due to a faster the uptake by the alveolar macrophages (100). Translocation of nanoparticles post inhalation to other organs like central nervous system via olfactory neurons is of particular concern (101) even though the translocation is highly dependent on the type of nanoparticle, size surface charge and the bio corona particles might acquire in contact with the nasotracheal mucus (94). The fiber – like shape of carbon nanotubes raised concerns over respiratory exposure to this nanomaterials and the possible asbestos like behavior with the induction of mesothelioma (102). Studies showed that even if the translocation to subpleural area of multiwall carbon nanotubes is possible (103) this might be dependent on batch to batch or provider (104) variation of the characteristics of the materials. Furthermore, possible enzymatic degradation of the single wall carbon nanotube (105) might be reducing the inflammatory process post exposure to these materials.

Healthy skin is an effective barrier for the entry of nanoparticles but in special conditions as sunburn or diseases the translocation of nanoparticles (106) via Langerhans cells to lymph nodes and to blood is possible. The exposure to TiO_2 or ZnO_2 nanoparticles via sun creams can result in translocation of the nanoparticles via the more permeable barrier of sunburned skin (107).

A wide variety of nanoparticles are used in food industry from Ag nanoparticles in food packaging, amorphous SiO_2 and PS as food additive, titanium dioxide (TiO2), gold (Au), platinum (Pt) and zinc oxide (ZnO) nanoparticles in cosmetics, especially sunscreens and toothpastes (108). Exposure to 50 nm polystyrene carboxylated nanoparticles in chicken induced inhibition of iron transport after acute exposure. A chronic exposure induced morphological changes in the intestinal villi to increase the surface area available for iron absorption. Also systemic effects like an increase of the coagulation time suggests also lipophilic vitamins deficiencies (vitamins A, D, E, K) (109).

In different diagnostic or therapeutic formulations, the nanoparticles can be exposed to blood via i.v. injection. Within the biological fluid the nanoparticles will rapidly acquire a corona of bio – molecules that will influence the biokinetics and the

interactions between the nanoparticles and the biological systems. For a more detail description of biocorona see 1.6.

1.5.2 Interaction of nanomaterials with immune system

The primary function of the immune system is to protect against foreign material (micro – organism, particles) to enter the organism. The innate immunity and the adaptive immunity are part of the immune system to protect against foreign intruders (Figure 6) (110).

Macrophages are professional phagocytic cells and important for removal of cell debris and foreign material. Dendritic cells (DCs) are antigen – presenting cells and orchestrate adaptive immune responses.

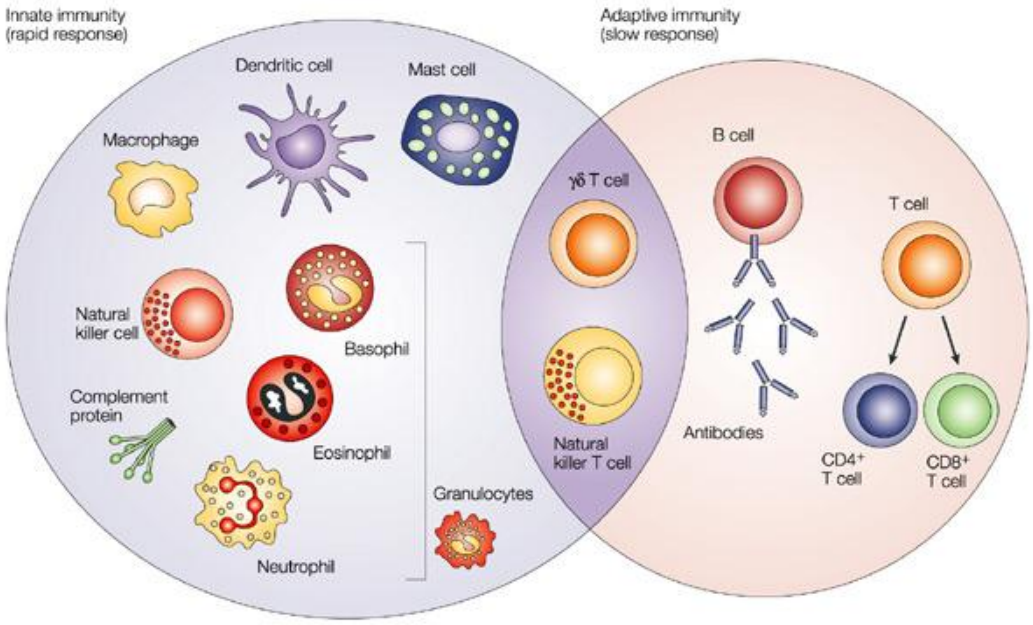

Figure 6. Innate and adaptive immune system (110)

Upon contact with blood and formation of bio – corona, nanoparticles might interact with red blood cells and thrombocytes involved in blood coagulation. In vitro exposure to human whole blood to gold nanoparticles (30 nm and 50 nm) did not cause delays in coagulation time or platelet aggregation (111). Studies on polyvinyl chloride resin particles (112) showed the effect of polyethylene glycol (PEG) coating as after the

coating the increase of the coagulation time, platelet aggregation in the presence of polyvinyl chloride resin were not observed.

The biochemical cascade known as complement system has as function the removal of the pathogens. The complement can be activated by the physical and chemical characteristics of the nanoparticles: size, shape, surface charge as well as composition (113, 114). Strategies like coating with PEG (115) or with polysaccharides (116) to avoid the complement activation by the nanoparticles showed that the complement activation is highly sensitive not only to the coating molecules but also on their density on the surface and the induced conformational changes.

The production of specific antibody (antigenicity) upon contact with nanoparticles as well as the production of cytokines is another response from the immune system. B cells production of antibodies can be in response to either nanoparticles themselves or to the functional groups or biomolecules attached on the surface (117). The size and the surface properties of the nanoparticles are important factors in determining the type of immune response (118, 119). In the event of inflammation, the immune cells are activated and secretion of cytokines (signaling molecules) is triggered. The positively (120) and neutral charged particles seem to trigger more the cytokine production compared to positively charged particles (ref). An increased immune response to nanoparticles as PMMA nanoparticles (121) or 200 nm amylopectin and maltodextrin nanoparticles (122) compared to the aluminum phosphate adjuvant render them applicable as adjuvant in vaccine strategies.

There is an emerging understanding that most of the toxicity effects exhibited by the nanoparticles as well as the interactions with the immune system are due to the presence of the biological corona on the surface of the nanoparticles.

1.6 NANO – BIO INTERACTIONS

Nanoparticles are endowed with a synthetic identity which comprises of a specific morphology (size and shape), chemical composition as well as surface properties (chemical reactivity, charge, roughness) (123). But will the cell "see" any of these intrinsic features? Or rather the cell will "sense" a completely new biological identity (with a new size and shape – determined by the attachment of the biomolecular corona

and possible induced/decreased agglomeration, a new surface charge) that will determine the possible interactions with the biological systems (124)?

1.6.1 Role of bio – corona

When nanoparticles, either accidentally or as part of different formulations for biomedical applications, come in contact with the nanoparticles enter in contact with physiological media, they encounter a complex environment that contains a huge variety of molecules with different functions: proteins, carbohydrates, nucleic acids and lipids (125). The biomolecular corona formation is a primary phenomenon at the interface between biological liquids and nanoparticles surface that will influence how the particles will initiate various reactions from the biological system and consequently will affect the fate of the particles (126) (127).

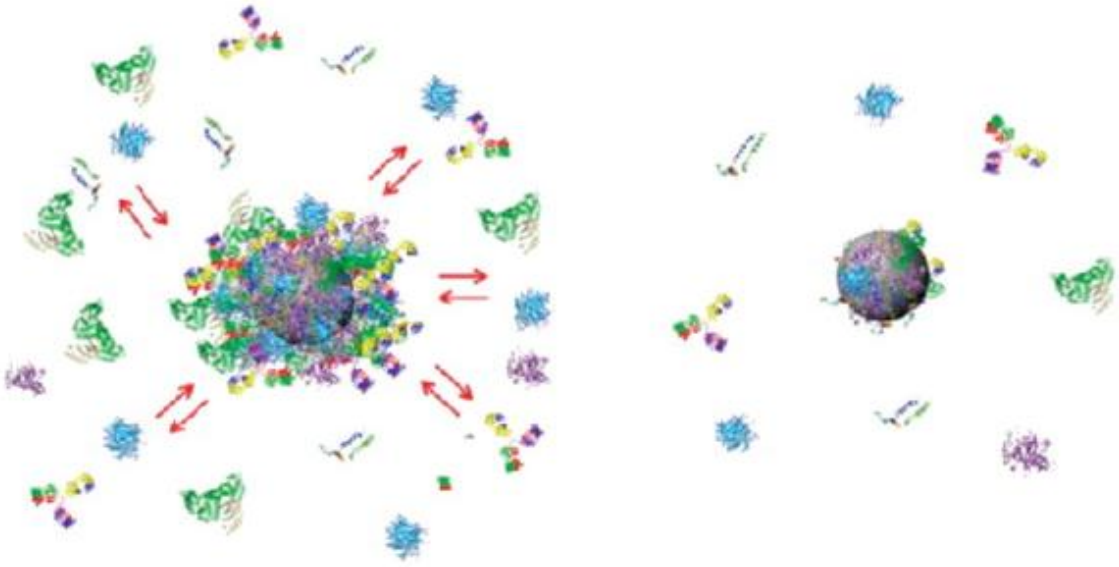

Figure 7. Schematic drawing of the structure of protein–nanoparticle: an outer layer of proteins (full red arrows) and a hard slowly exchanging corona of proteins (right) (124)

Studies on different types of nanoparticles reflect the biomolecular corona formation as a dynamic phenomenon. The Vroman effect (128-130) seems to dominate the dynamic of the formation of the corona on the nanoparticles surface, resulting in a competitive adsorption to a relatively small numbers of adsorption sites. The molecules with a higher mobility and abundance will absorb in initial stages being replaced later by molecules with higher affinity for a specific surface. The adsorption of biomolecules is driven by the surface dependent properties as surface charge, hydrophibicity/hydrophilicity (131). The size of the nanoparticles plays an important

role as the surface area available for interaction with the media is a limiting factor (132). It is generally accepted that immediately after the contact with the biological media, an initial corona is formed by the loosely bound low affinity proteins. A prolonged incubation allows the formation of denser, irreversibly attached, "hard" corona from high adsorption affinity proteins (133, 134) and a satellite "soft" corona that encounters intensive exchanges with the surrounding media (135). The "hard" corona is formed due to the direct interaction of the proteins with the surface of the nanoparticles while the protein-protein interactions dominate the exchanges interactions of the "soft" corona with the "hard" corona (124). The time scale of the process probably is very short with a stable corona formation after as short as 30 seconds (136). Relevant for *in vivo* fate of long circulating nanoparticles might be the "hard" protein corona that is strongly attached to the surface of nanoparticles and resist to events as translocations through biological membranes (137). Furthermore, changes in the "hard" corona might occur when the particles are transferred to another biological compartment with a different biomolecular profile (137).

Regardless the way the nanoparticles enter the body and the biological identity they acquire upon interaction with various biological media they will finally interact with the cells membrane, and they will have a degree of impact on the cellular function. In this thesis, the impact of nanoparticles with/without a corona of plasma proteins is investigated (Paper III).

1.6.2 Safety by design

Going back to the chemistry lab and trying to design a "perfect" nanoparticle one would have to think how the physical and chemical parameters affect their performances when applications in nanomedicine are envisioned. Part of the designing process of a "safe" nanoparticle the formation of the protein corona and its possible in vitro and in vivo implications needs to be addressed.

Size. The size of the nanoparticles is not important just because they are in same dimensions range with biological molecules but also because of the increased surface area and increased constituents atoms exposed to the surface. Regarding protein adsorption size might be important as smaller sizes (under 30 nm) might induce a reduction of the protein adsorption (138) due to space restriction and consequent steric hindrance. An increase in size is reflected by increasing protein coverage (134, 139).

Furthermore, the possible induced agglomeration of the nanoparticles by the protein coating might change the effective surface area and might induce undesired in vivo effects as infarctisation of small capillary.

Surface properties. The interaction between the particles and the cells surface or biological membranes (negatively charged) might be influenced by the zeta potential of the nanoparticles (140). Additionally, the surface charge seems to play an important role in biocorona formation, with more proteins binding to more charged particles (141) than the neutrally changed surfaces (142). An increase in the protein adsorption to the nanoparticles surfaces is observed on the more hydrophobic nanoparticles as compared to the hydrophilic nanoparticles (143). The formation of a protein corona might trigger opsonisation and eventual fast clearance from the blood stream, lowering the chance that the particles will reach the target sites/cells to achieve their goal. Furthermore, activation of the complement cascade and coagulation cascade will trigger immune and systemic undesired responses. Consequently strategies that would minimize protein adhesion to the surface of the nanoparticles has to be included in the design. Antifouling coating with long chain polymers like PEG (127) or polysaccharides (144) induce a reduction of protein adsorption and consequently a reduce interaction with immune system.

Particle chemistry and crystalline structure. Chemically stable nanoparticles are preferred for most applications. The release of ions in liquid media (as ZnO nanoparticles) with potential toxic effects (140), or the surface oxidation of particles (145) in different media might trigger different toxic and immune effects. For some materials, the toxicity depends on its type of crystalline form (146): 200 nm nanoparticles TiO_2 rutile induced oxidative DNA damage while the effect was not observed for the same size nanoparticles but anatase crystalline structure.

2 AIMS OF THE STUDY

The aims of the whole study are divided chronologically in:

- To synthesize engineered core-shell nanoparticles with single iron oxide core and finely tunable silica shell with a narrow size distribution as contrast agents for MRI.

- To investigate the effect of SPIONs with different surface coatings (silica versus dextran) and different sizes on immune cells (human primary macrophages and human primary dendritic cells): on in vitro biocompatibility and cellular internalization.

- To determine how the surface of SPIONs (silica versus dextran) affects the composition of the corona of human plasma proteins and the subsequent in vitro behavior of the nanoparticles.

- To synthesize homogeneous, transparent 3D nanostructures with iron oxide nanoparticles dispersed in PMMA matrix via in-situ polymerization for magneto-optic applications.

3 MATERIALS AND METHODS

Detailed description of the materials and techniques used in our studies can be found in the publications and manuscripts included in the thesis. The sections below provide a summary of the methods and their basic principles.

3.1 SYNTHESIS

3.1.1 Magnetic nanoparticles

SPION and thermally blocked nanoparticles were prepared by high temperature decomposition of an iron precursor: iron oleate - Paper I, Paper III and Paper IV or iron oxyhydroxide - Paper II. Both syntheses are high temperature decomposition synthesis in a high boiling temperature organic solvent (oleic acid) that enables accurate control of the size of the obtained iron oxide nanoparticles. The resulting particles have a surface capping of oleic acid, readily dispersible in organic solvents. Even though the method that is using iron oleate as precursor (31) is a two steps method, the nucleation and growth is homogeneous as the precursor is a solution. Using iron oxyhydroxide (FeO(OH)) as precursor (33, 34) is a one – pot method in which the dissolution of the precursor, formation of iron oleate complex and thermal decomposition at elevated temperatures is taking place successively by heating up the mixture. In this method, the separation of the nucleation and growth process from the formation of iron oleate precursor is not so effective and consequently, obtaining monodispersed iron oxide nanoparticles is difficult to control.

3.1.2 Core – shell nanoparticles (CSNPs)

The SPION obtained by both methods were subsequently coated with silica shell by the inverse microemulsion method in a Triton X100/hexanol/water/cyclohexane system (Figure 8). The microemulsion system is recognized as an effective way of controlling the size of the particles. Even though the obtained particles are highly monodispersed, the unreacted precursor creates aggregation during the destabilization of the microemulsion and collection of the particles. The introduction of two supplementary steps in the post synthesis process: (*i*) pH adjustment to approximately 2 and (*ii*) successive cycles of liquid N_2 cooling, improved dramatically the quality of the obtained core shell nanoparticles. (Paper I, Paper II)

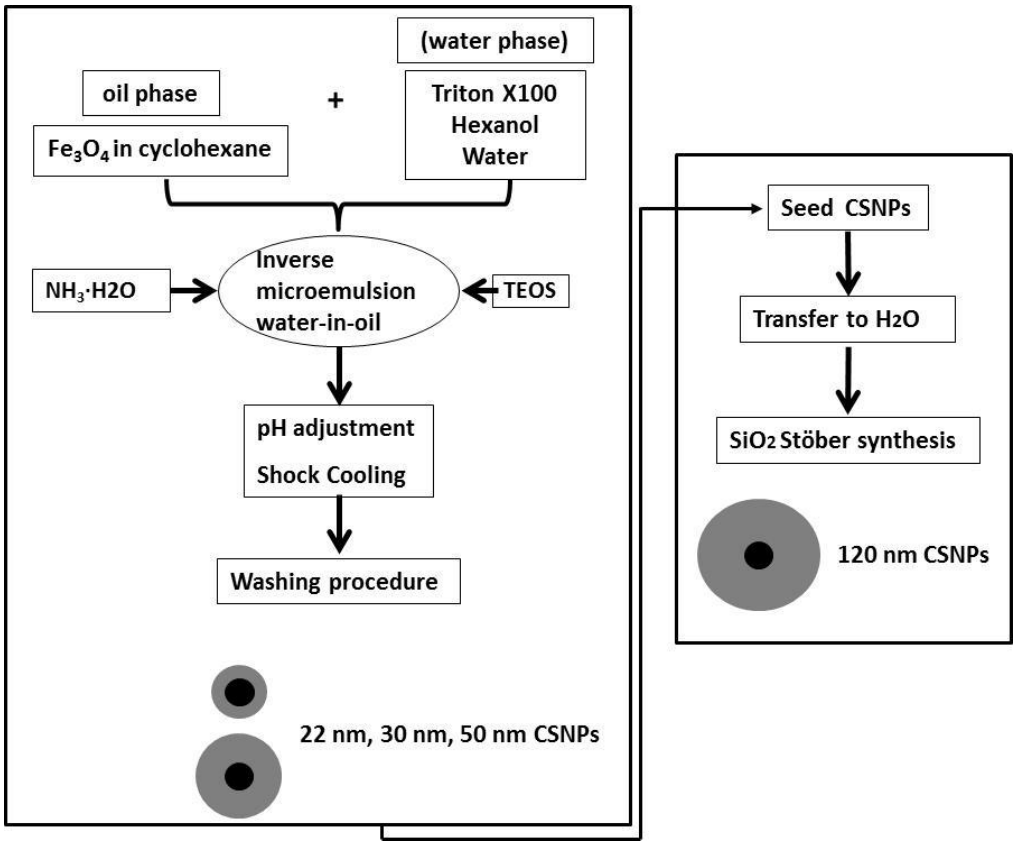

Figure 8. Schematic of the CSNPs synthesis by inverse microemulsion and Stöber method

The size of the water phase droplets is the limiting factor of the growth of the particles in the inverse microemulsion system. The increase of the particles size over a certain value will have as consequence a decreased stability of the microemulsion. This fact will have as effect a broadening of the size distribution of the resulting particles. Consequently, the seeded particle growth using Stöber method (147) (Figure 8) was utilised for obtaining core-shell nanoparticles with larger size (Paper II, Paper III). As seeds CSNPs with average diameter of ~30 nm were used which were obtained through silica coating in inverse microemulsion. The thickness of the silica layer is controlled by the amount of the silica precursor added, the other variables (the seeds concentration, water to alcohol ratio, quantity of ammonia, reaction time) being maintained constant.

3.1.3 Magnetic nanocomposites

Several chemical approaches have been developed to prepare nanocomposites of nanoparticles and copolymers. In the two step approach used in Paper IV the nanoparticles are prepared first followed by chemical polymerization of the polymer

around the particles (148, 149). The use of organic dispersible nanoparticles and sonication as method for dispersing the fillers in the monomer matrix results in homogeneous nanocomposites.

3.2 PHYSICAL AND CHEMICAL CHARACTERISATION METHODS

The fabricated materials (SPIONs cores and CSNPs) as well as the commercial dextran coated SPIONs (nanomag®-D-spio) were analyzed at various stages of the synthetic process and during the biocompatibility assessments using a large variety of techniques described as follow.

Atomic absorption spectroscopy (AAS) and Inductively Coupled Plasma (ICP). The amount of iron oxide nanoparticles in cyclohexane suspension and of iron oxide core – silica shell composites in the final water suspension was measured by AAS (Paper I) and ICP (Paper II, Paper III, Paper IV).

The basics principle of both techniques relies on the fact that atoms emit characteristics electromagnetic radiation (hv) as they relax from an excited state to their ground state. The main differences between these two techniques are the source of energy used for the excitation of atoms: flame (1500–2500 °K) and plasma (4000–8000 °K) and related to this is the ionization efficiency and the detection limit (ppm – AAS, ppb – ICP). Another important advantage is the possibility to analyses multiple elements in one run for ICP whereas AAS measurements are limited to one element at a time.

The sample preparation for these techniques consists of complete removal of the sample from its original matrix in order to minimize interferences which practically means digesting the sample with a strong acid. Both techniques require the use of standard solutions for calibration curves in order to perform quantitative analysis.

Electron Microscopy. In any type of microscopy, the image is formed as a result of the interaction of the incident particles with the samples. In electron microscopy, when the particles (electrons) hit the sample, different interactions can occur. These interactions and the generated signals are the basis of the various imaging and spectroscopy methods that can be utilized in electron microscopy. From the incident electron beam only a small part is passing through the sample with the energy unchanged. Most of the incident electrons will have their initial energy reduced as a result of inelastic

interactions (X-rays, Auger electrons, secondary electrons, plasmons, phonons, UV quanta or cathodoluminescence) (Figure 9). A small part of the electrons will have their energy preserved but their trajectory will be modified as a result of elastic interaction with the sample.

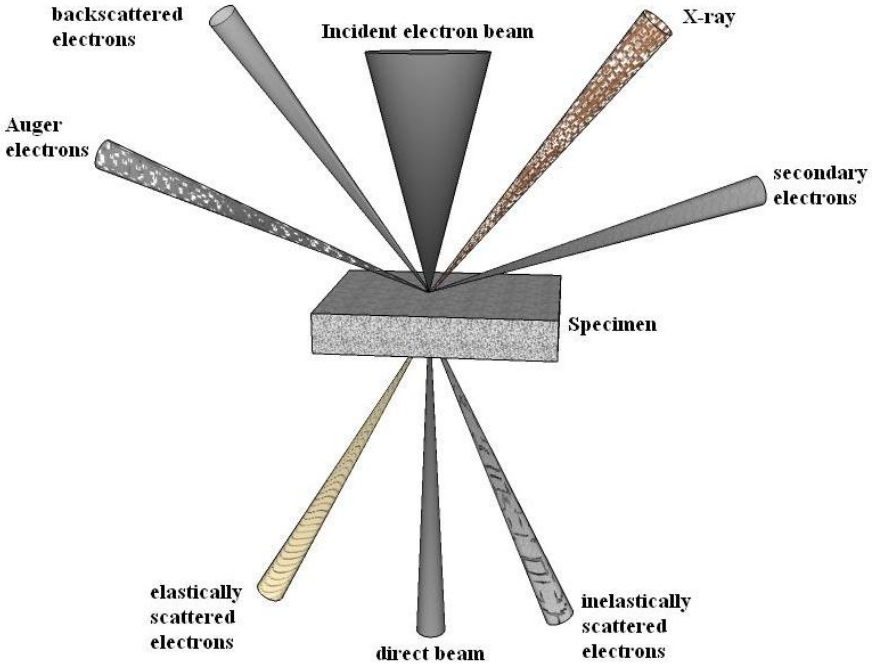

Figure 9. Scheme of electron-matter interactions arising from the impact of an electron beam onto a specimen.

Transmission electron microscope (TEM). In TEM the transmitted electrons through the thin sample are used to form a map of local densities and diffraction information (ED) when crystalline samples are analyzed. The morphology, size and size distribution study of the iron oxide cores and iron oxide core – silica shell nanoparticles were investigated with transmission electron microscope (TEM).

Scanning electron microscopy (SEM). The possibilities of analyzing just very thin specimens on a very small area are important limitations of the TEM. These constraints were the incentives for developing electrons microscopes that can analyse bulk (thick) samples on a much larger area - SEM. In SEM, as in TEM, the dual character of electrons (charged particles and wave) is exploited to image the sample. The beam of primary electrons is scanned across the specimen simultaneously in two perpendicular directions covering a square/rectangular area of the sample (raster). Collecting the secondary electrons from each point of the sample an image can be formed.

Fourier Transform Infrared Spectroscopy (FTIR). The study of the surface of the particles is performed using FTIR analysis.

FTIR is based on the fact that most molecules absorb light in the infra-red region of the electromagnetic spectrum (0.8 μm to 1 mm wavelength), this absorption corresponding specifically to the bonds existing in the molecule. The sample is irradiated with a broad spectrum of IR light and the absorbance at particular frequencies is plotted after the data is treated with a Fourier transformation. The resulting spectrum is a fingerprint of a sample with absorption peaks that correspond to the frequencies of vibrations between the bonds of the atoms in the molecule. The analysis of the samples is done either in solid (dry) or colloidal form. Due to the Attenuated Total Reflectance (ATR) crystal in the structure of the FTIR, no sample preparation is required (apart from evaporating the solvent to obtain the dry powder when the study is done in dry form).

X-ray powder diffraction (XRD). When radiation hits a sample, it is either scattered (in an elastic manner or inelastic) or absorbed. When the scattering is entirely elastic, the energy of the primary radiation remains unchanged, no energy being lost. The regular arrangement of the atoms in a crystalline material interacts elastically with the radiation that has the wavelength comparable with the interatomic distance. The principle of XRD powder diffraction is based on the elastic interaction of the X ray radiation with samples. X-rays are produced with wavelengths matching the unit cell dimensions of crystals (10^{-10} m). The result is a diffraction spectrum in which the intensity of the scattered radiation is plotted as a function of the scattering angle. The diffraction angles and the diffraction intensities are a function of the crystal structure.

The diffraction pattern obtained by XRD powder diffraction can help in identifying the phase composition of a sample, in calculating the unit cell lattice parameters and the crystallites sizes but can also give information about residual strains (macro or micro-strains).

Dynamic light scattering (DLS). When particles are dispersed in a liquid medium they undergo Brownian which causes the fluctuations of the local concentration of the particles, resulting in local inhomogeneity of the refractive index. DLS is determining the velocity distribution of particles movement by measuring dynamic fluctuations of

intensity of scattered light. With the assumption that the particles are spherical and non-interacting, the mean radius is obtained from the Stokes-Einstein equation

$$R = \frac{k_B BT}{6\pi\eta D} \qquad (4)$$

where R is the hydrodynamic radius, k_B is the Boltzmann constant, T the temperature, and η the shear viscosity of the solvent.

The sample temperature is important, as is directly proportional to the radius value but also because viscosity of the solvent is directly dependent to the temperature. Most importantly, the particle size determined by dynamic light scattering is the hydrodynamic size, which is the size of a spherical particle that would have a diffusion coefficient equal to that of our particles.

Zeta potential measurements. The development of a net charge at the particle surface affects the distribution of ions in the surrounding interfacial region, resulting in an increased concentration of counter ions (ions of opposite charge to that of the particle) close to the surface. Thus an electrical double layer exists around each particle. The liquid layer surrounding the particle has an inner region, called the Stern layer, where the ions are strongly bound and an outer, diffuse, region where they are less firmly attached. Within the diffuse layer there is a notional boundary inside which the ions and particles form a stable entity which will move together with the particles. The potential that exists at this boundary is known as the Zeta potential. When an electric field is applied across an electrolyte, charged particles suspended in the electrolyte are attracted towards the electrode of opposite charge. By determining the Electrophoretic Mobility it is possible to calculate the zeta potential of particle.

Termogravimetric analysis (TGA) and Differential scanning calorimetry (DSC). Both techniques are thermal analysis studying the change in properties of the materials with temperature. DSC is thermoanalytical technique in which the difference in the amount of heat required to increase the temperature of a sample and reference is measured as a function of temperature. The basic principle of the techniques is that the physical transformation of a sample is reflected in the heat exchange necessary to maintain the sample at the same temperature as the reference. It can detect exothermic and endothermic processes but also more subtle processes as glass transitions. TGA

determines changes in weight of the sample in relation to a temperature program in a controlled atmosphere.

Ultraviolet – visible spectroscopy (UV–Vis). Ultraviolet and visible (UV-Vis) absorption spectroscopy is the measurement of the attenuation of a beam of light after it passes through a sample. Ultraviolet and visible light are energetic enough to promote outer electrons to higher energy levels. UV-Vis spectroscopy is usually applied to molecules or inorganic complexes, as well as nanomaterials having absorption in this wavelength region.

3.3 MAGNETIC CHARACTERISATION METHODS

Vibrating sample magnetometer (VSM). VSM uses an induction principle, and is widely used for characterizing the magnetic properties of materials. If a sample of any material vibrates with sinusoidal motions in a uniform magnetic field a sinusoidal electrical signal (a current or voltage) will be induced in a sensing coil. The electrical signal has the same frequency as the vibration frequency of the sample and its amplitude is proportional to the magnetic moment. VSM measures permanent moments and hysteresis curves of materials. The fitting of the profiles gives several parameters as the crystal radius (r) and the specific magnetization (M_S).

Magnetic resonance (MR) relaxometry measurements. The fundamental principle of MR relaxometry is identical with the MRI principle (1.4.). The ability of the agent to reduce the T_1- and T_2- relaxation times are respectively described by the R_1 (1/ T_1) and R_2 (1/ T_2) relaxation values of the agent and is defined by:

$$R_{1,2} = R^0{}_{1,2} + r_{1,2}C \qquad (5)$$

where $R_{1,2}$ (unit s^{-1}) is the respective T_1 or T_2 proton relaxation rate in the presence of the contrast agent, $R°_{1,2}$ are the relaxation rates in the absence of contrast agent and C is the contrast agent concentration (unit mM). The constant of proportionality $r_{1,2}$ (unit s^{-1} mM^{-1}) is called relaxivity and is a measure of the increase in the relaxation rate of protons per unit concentration of contrast medium (150).

Alternating gradient magnetometer (AGM). AGM measures the magnetic moment of a sample by measuring the force on a magnetic dipole by a magnetic field gradient. It is a very sensitive method, a factor of 10^2 more sensitive than VSM. The sample's

size and mass necessary for measurements in AGM are less than in VSM, but the measurements are limited to solid samples (151).

Faraday rotation (FR) measurements. Faraday rotation is a magneto-optical phenomenon that causes a rotation of the plane of polarization, rotation that is linearly proportional to the component of the magnetic field in the direction of propagation. Consequently, Faraday rotation is an important property that couples the optical and the magnetic behavior of a material. The magnitude of this effect depends on the sample magnetization, the wavelength of light used and the length of the sample crossed by the light. Materials that have a high FR effect find applications in optical telecommunications and other laser applications (152).

3.4 CELL ISOLATION AND CULTURE

Density is a basic material characteristic defined as mass per unit volume. Blood is a liquid tissue composed of approximately 55% fluid plasma and 45% cells. The average density of whole blood for a human is about 1060 kg/M^3. The density of blood plasma is approximately 1025 kg/m^3 and the density of blood cells circulating in the blood is approximately 1125 kg/m^3. Centrifugation is applied to the whole blood in order to separate the different components: erythrocytes, buffy coat (containing 90% of the leukocytes from the whole blood and 70-90 x10^9 platelets) and plasma. In order to separate agranulocytes (lymphocytes and monocytes) from the granulocytes (neutrophils, basophils and eosinophils) a density gradient centrifugation is applied using as sedimentation medium (Lymphoprep or Ficoll-Pacque). Further selection of the monocytes from the leucocytes population is performed based on their differential expression of Cluster of differentiation 14 (CD14) proteins on their membrane.

3.4.1 Primary dendritic cells

Dendritic cells (DC) are antigen-presenting cells (APCs) which play a critical role in the regulation of the adaptive immune response. One approach to generate DC is by culturing CD14+ monocyte-enriched peripheral blood mononuclear cell (PBMC) in the presence of Granulocyte-macrophage colony-stimulating factor (GM-CSF) and IL-4 (153). An additional 3 days "maturation culture" step in the presence of GM-CSF and IL-4 is necessary to generate fully mature dendritic cells. Cluster of Differentiation 1a (CD1a), complement component 3 receptor 4 subunit (CD11c), CD14 and Cluster of Differentiation 83 (CD83) are all surface proteins found in the

dendritic cells membranes and markers for the successful in vitro differentiation of this type of cells from monocytes (154).

3.4.2 Primary macrophages

Macrophages are phagocytic cells with function in both non-specific defense (innate immunity) as well as help initiate specific defense mechanisms (adaptive immunity) of vertebrate animals. The monocytes differentiate in vitro into macrophages by culturing in medium containing macrophage colony-stimulating factor (M-CSF) that induces differentiation of the monocytes into macrophages (155). CD14, CD68 and/or mouse F4/80 or human epidermal growth factor module-containing mucin-like receptor 1 (EMR1) are widely used as macrophage-specific markers (156).

3.5 CELLULAR TOXICITY ASSESSMENT

3.5.1 Limulus Amebocyte Lysate (LAL) test

LAL test detects and measures bacterial endotoxins as Lipopolysaccharides (LPS), found in the outer membrane of Gram-negative bacteria. LPS is an endotoxin that induces a strong response from normal animal immune systems. Furthermore, LPS promotes the secretion of pro-inflammatory cytokines in many cell type by binding the CD14/TLR4/MD2 receptor complex. Consequently is extremely important that all the nanoparticles are tested for LPS contamination before undergoing any type of biocompatibility tests (157). The method used in Paper II and Paper III is an end – point chromogenic assay, monitoring the appearance of yellow colour, which is directly related to endotoxin concentration in the sample. Endotoxin levels in unknown samples are determined by comparison to a standard curve.

3.5.2 MTT test

To test the mitochondrial activity of the macrophages as a measure of cell viability after exposure to nanoparticles, MTT is a common method used. This is a colorimetric assay that measures the reduction of yellow 3-(4,5-dimethythiazol-2-yl)-2,5-diphenyl tetrazolium bromide (MTT) by mitochondrial succinate dehydrogenase. The MTT enters the cells and passes into the mitochondria where it is reduced to an insoluble, colored (dark purple) formazan product. The cells are then treated with an organic solvent and the formazan product is released. Since reduction of MTT can only occur in metabolically active cells the level of activity is a measure of the viability of the cells (158). The assay is convenient as it can be adapted to a 96 – well plate format.

3.5.3 Trypan blue exclusion

Trypan blue (called because it can kill trypanosomes) is derived from toluidine. Live cells possess intact cell membranes that exclude certain dyes, such as trypan blue, Eosin, or propidium, while the membrane of the death cells is permeable to these substances (blue cytoplasm). Because the alive cells are excluded from staining (clear cytoplasm), this method is called dye exclusion method (159). The method though cannot distinguish between necrotic and apoptotic cells. Cells are evaluated by light microscopy.

3.5.4 Annexin V/Propidium Iodide staining

In the early stages of apoptosis changes occur at the cell surface such as the translocation of phosphatidylserine (PS) from the inner side of the plasma membrane to the external surface of the cell. Annexin V, a protein with high affinity for PS, can be used as a sensitive probe for PS exposure upon the cell membrane. Furthermore, the exposure of PS to the external surface of the cells, occurs also in necrosis. Because the main difference between early stages of apoptosis and necrosis is the cellular membrane integrity, the measurement of Annexin V binding to the cell surface has to be performed together with a dye exclusion test that establishes the membrane integrity (160, 161). Consequently, the cells that PI−/Annexin V+ are defined as being in early apoptosis whereas cells with PI+/Annexin V+ are counted as late apoptotic or secondary necrosis. Determination of annexin V binding is performed by flow cytometry or Fluorescence Activated Cell Sorting (FACS). FACS is a method used for the evaluation of cell-membrane proteins, intracellular proteins as well as peptides and DNA. The basic principle behind FACS is an antigen-antibody reaction, where the antibodies are fluorescently labeled. In a FACS analysis a labeled colored suspension of cells passes a focuses laser beam where the label is stimulated. The emitted florescent light from the flurophores, which are coupled to the antibodies, and the scattered-light are detected separately.

3.6 CYTOKINE SECRETION

In the event of inflammation, cells of the immune system are activated. Nanoparticles are recognized the immune cells due to their surface properties and composition, and eventually an immune response is mount. Consequently, the immune cells are responding to the presence of nanoparticles in the same way as to the presence of a pathogen or a foreign substance, by releasing chemical messengers (mostly proteins)

called cytokines (117, 162, 163). Enzyme-linked immunosorbent assay (ELISA) is an enzymatic assay that uses antiboby – antigen reaction. It can be used either to detect the presence of proteins recognized by an antibody or to test for antibodies that recognize an antigen (the variant used in our studies).

3.7 ASSESSMENT OF CELLULAR UPTAKE

3.7.1 Qualitative assessment

Electron microscopy, besides being an important tool for characterization of materials, is important for the comprehensive identification of the nano-bio interactions. TEM facilitates in depth analysis of the morphology and functional state of the cells following the uptake of nanomaterials. Furthermore, TEM can provide evidence of nanomaterials being / or not encapsulated in nanocarriers and their intracellular localization based on their high electron density (164, 165). Due to the use of ultrathin sections (50 – 100 nm) the technique provides a high-resolution visualization of the internal structure of the cells with the price of losing the dimensional information for structures bigger than the thickness of the section. Another important factor to remember in analyzing TEM images is the variability of the images imposed by the inherent inhomogeneity and anisotropy of the biological structures (166).

3.7.2 Quantitative assessment

Inductively coupled plasma mass spectrometry (ICP-MS) is a highly sensitive method that can measure concentrations below one part in 10^{12} (part per trillion) of analytes. The method is coupling the ICP for ionization of the elements with mass spectrometer for separation and detection of ions. Due to its high sensitivity and very low detection limit the method ICP-MS is used for quantification of cellular uptake of nanoparticles. Even though is an excellent quantitative tool, it is a destructive technique, prior digestion of the cells and dissolving of nanoparticles being part of the sample preparation in order to separate the analytes from the matrix. Furthermore, the technique cannot differentiate between internalized or just adsorbed on the cellular membrane nanoparticles (165, 167, 168).

3.8 PROTEOMIC ASSESSMENT OF BIO – CORONA

Two main approaches are used in mass spectrometry based proteomics. In top – down proteomics the intact proteins are analyzed. However, the most common design of the proteomic assessment of the bio – corona by mass spectrometry is a bottom – up approach. This approach, also known as shotgun proteomics, is based on enzymatic cleavage of proteins into peptides, usually by trypsin, to facilitate the ionization and fragmentation for the subsequent identification of the proteins.

When assessing the biocorona acquired by the nanoparticles in a biological environment, prior MS measurements, a thermal and chemical denaturation of the proteins is performed using a surfactant in low concentrations. Apart from denaturation by disrupting the hydrogen, hydrophobic and electrostatic bonds of the proteins, the surfactant is disrupting the same type of interactions of the proteins with the nanoparticles surface. Two mains methodologies are then used for obtaining the peptides that will be submitted form MS. One approach is using an intermediate step of separating by 1D electrophoresis. Following an in gel digestion, the peptides are subjected for analysis to MS (169). The other approach is the on - particles digestion approach where the proteins are denatured, reduced, alkylated and trysinised directly from the surface of nanoparticles without the intermediate step of in gel trypsinisation (170).

3.8.1 Mass spectrometry

Mass spectrometry is a central analytical technique for protein research and for the study of biomolecules in general (171, 172).

A mass spectrometer consists of an ion source, a mass analyzer that measures the mass-to-charge ratio (m/z) of the ionized analytes, and a detector that registers the number of ions at each m/z value. The peptides are separated according to their mass, partially fragmented in amino acids and then by combining the fragmentation data with the mass data obtained, the amino acid sequence of each peptide is obtained. The identified peptide masses are then searched against a protein database of in silico digested peptides to match, based on the characteristic mass of a peptide with a certain sequence, the peptides with known proteins(172). Prefractionation by chromatographic separation is applied prior MS analysis to the mixture of peptides obtained after the trypsinisation

of the proteins to reduce the complexity of the peptide mixture and to increase the sensitivity of the technique.

A relative quantification of the proteins by MS (comparing individual peptides/proteins between the experiments) is done either label free or using isotopic labeling. The advantage of using isotope labeling is the possibility to pool the samples so that the technical variability is reduced, the quantitative analysis being performed in one spectrum and not between several spectra.

3.8.2 Bioinformatics

The results from a mass spectrometry based proteomics are a long list of identified and/or quantified proteins. In order to translate these results into functional analysis and other possible biologically relevant analysis, the use of bioinformatics tools is necessary. Bioinformatics analysis starts with a matrix or sheet of quantitative measurements of protein levels expressed as peptide counts from the mass spectrometer. Rows in the matrix denote proteins and columns represent samples, such as protein corona from certain nanoparticle.

Statistical tests, such as t-test, can then be used to determine which proteins are differentially bound to various types of nanoparticles. In order to be applicable, sufficient numbers of biological replicates need to be present. Statistical tests are an example of supervised methods of analysis because external information about the samples is used to predefine classes of observations. Clustering analysis is a set of techniques that seeks to divide the data into groups based on the patterns inherent in the data itself and can be termed an unsupervised method of data analysis. Hierarchical clustering starts from the bottom up to connect most similar observations together and proceeds to connecting groups or clusters of observations together to build up a tree where the most similar observations or proteins are close together. Other methods such as k-means, self organizing maps (SOM) or partitioning around medoids (PAM) allot samples or proteins into predefined number of bins. The number of bins can be determined from the data itself or by trial and error.

Ontologies are structural frameworks used for organizing information in a domain using a common vocabulary and classifications to define objects, concepts and their properties and relations. Gene Ontology (GO) project consequently provides a

structured, precisely defined, common, controlled vocabulary for describing the roles of genes and gene products (proteins) in any organism (173). It is divided into three independent ontologies: molecular function (MF), biological process (BP) and cellular component (CC) (174) a protein being linked to one or several categories in the same branch.

KEGG (Kyoto Encyclopedia of Genes and Genomes) is another bioinformatics resource for understanding higher-order functional meanings and utilities of the cell or the organism from its genome information (174). KEGG describes mainly proteins interaction networks that are responsible for various cellular processes.

Groups of proteins obtained based on statistical analysis or clustering can be analyzed for the over-representation of certain classes of proteins. Over-represented classes of proteins, such as KEGG pathways or GO categories, describe the proteins from a set that appear more often than would be expected by chance alone, when using the so called hypergeometric test to calculate the odds. Thus using additional software (such as Ingenuity pathways analysis) can help organizing a set of proteins (for example the proteins identified in protein corona) into groups of molecular functions, biological processes, pathways to discover common features in the proteins of interest such as enrichment relative to a proteins set.

4 RESULTS

4.1 PAPER I. HIGH QUALITY AND TUNEABLE SILICA SHELL – MAGNETIC CORE NANOPARTICLES SYNTHESIS AND CHARACTERIZATION

In this study, synthesis of core – shell particles with a single core of iron oxide nanoparticle and tunable silica shell thickness via inverse microemulsion method is achieved. An investigation on the factors that affect the separation and monodispersity of the core shell particles and the growth of silica shell is conducted.

SPION nanoparticles with average size of 9.5 (±1.2) nm are obtained by the procedures described in 3.1.1 section. The High Resolution Transmission Electron Microscopy (HRTEM) images analysis matches the XRD measurements confirming that the nanoparticles composition is an iron oxide phase: either magnetite (Fe_3O_4) (ICDD#: 00-002-1035) and maghemite (γ-Fe_2O_3) (ICDD#: 00-013-0458) which have very close crystalline structure (spinel structure) and consequently is difficult to discriminate by this analysis.

SPION were used as core for the fabrication of core-shell nanocomposites in an inverse (water/oil) microemulsion Triton-X100/hexanol/water/cyclohexane system. The hydrophobic oleic acid capping on the surface of SPION make them easily dispersible in cyclohexane, which is the continuous phase (oil phase) of the next step in the synthesis process: the inverse microemulsion synthesis. Triton-X100/hexanol are used as surfactant / co-surfactant couple.

The hydrodynamic conditions were studied and no significant influence of the stirring rate on the size dispersion and homogeneity of core-shell nanoparticles formation was observed although it seemed to have an important role in the stability of the microemulsion system. Furthermore, we studied the variation of silica shell thickness as a function of time, the amount of TEOS and the SPION core size being maintained constant. For the identical set of initial conditions, the thickness of the silica shell increases linearly with time, reaching a constant value after 17h and remaining almost constant if the reaction time is further increased.

One important drawback of the microemulsion method is the fact that the resulting core-shell nanocomposites are strongly necked due to residual reactions leading to formation of silica layer connecting particles together (40, 49, 50, 52, 53, 175). A combination of two pH adjustment of the aqueous phase in the pH range of 1-2 (176) and the kinetic destabilization of the microemulsion by shock cooling highly separated, non-aggregated magnetic core - silica shell nanoparticles were obtained.

A comprehensive magnetic characterization was performed on the core – shell nanoparticles with different silica shell thickness. The core-shell nanocomposites retained the superparamagnetic character of the magnetic core particles, the magnetization per unit weight of sample decreasing as the thickness of the silica shell is increasing for the same magnetic core size of SPION. Relaxivity studies performed on the core – shell particles revealed values for the r_2/r_1 ratios of ~ 3.5 fold higher than those of Resovist at 0.47T (20 MHz) and ~ 6 times higher than those of Feridex at 0.47T (20 MHz) which indicates higher T2 contrasting characteristics of the core shell suspensions.

In summary, we successfully synthesized core–shell nanoparticles with a narrow size distribution, a crystalline magnetic core and a tunable amorphous, porous silica shell thickness. The carefully adjusted post-synthesis processing resulted in core–shell nanoparticles highly separated, with no residual aggregation. Magnetic measurements showed a superparamagnetic character with sufficiently high magnetization, rendering them useful for biomedical applications as biomedical targeting and imaging (e.g. magnetically driven drug delivery systems, MRI contrast agents, cell separation, etc.).

4.2 PAPER II. EFFICIENT INTERNALISATION OF SILICA - COATED IRON OXIDE NANOPARTICLES OF DIFFERENT SIZES BY PRIMARY HUMAN MACROPHAGES AND DENDRITIC CELLS

In this study, an investigation is performed on the effect of the size and the surface coating of the SPION on the biocompatibility and intracellular internalization in human primary macrophages and human primary dendritic cells. De novo synthesized silica coated SPIONs (CSNPs) with overall diameter of 30 nm, 50 nm, 70 nm, and

120 nm were compared with cluster type dextran-coated iron oxide nanoparticles (nanomag®-D-spio) with two average sizes of the cluster of 20 nm and 50 nm.

The hydrodynamic diameter of the CSNPs increased upon incubation in cell culture media, compared to the diameter measured in deionized (DI) water, whereas the hydrodynamic sizes of nanomag®-D-spio samples remained similar in the two dispersion media. The surface charge on CSNPs and nanomag®-D-spio evaluated in DI water showed that CSNPs were negatively charged in the pH range of 4 - 9, reaching −22 mV at physiological pH. (124). Nanomag®-D-spio showed a small positive charge below pH 6.3, exhibiting surface potential of approximately −3 mV at physiological pH (177).

The superparamagnetic character of the core nanoparticles is retained in the case of nanomag®-D-spio nanoparticles and for CSNPs when the silica thickness increases although the value of the weight normalized Ms value is decreasing when the silica shell thickness is increasing. The r2/r1 ratios at 20 MHz obtained for CSNPs nanoparticles are higher when compared with reported values in the literature of commercially available T2 contrast while for nanomag®-D-spio the values are comparable.

Whereas the mitochondrial function in primary human macrophages and the cell vibility in primary dendritic cells are not affected upon incubation with nanomag®-D-spio, cellular type dependent results are obtained after incubation with various sizes of CSNPs. The mitochondrial function of primary human macrophages was decreased just when exposed to higher doses of 100 μg/mL, while an increase in cell death of the human dendritic cells was observed for smaller sized CSNPs (30 nm and 50 nm) in a dose dependent manner. The results indicate a higher sensitivity of the dendritic cells compared to macrophages when exposed to smaller particles. Additionally, the production of pro – inflammatory cytokines: TNF-α in both cell types, and cytokines IL-6 (human primary macrophages) or IL-12 (human dendritic cells) was not induced after incubation with the nanoparticles for 24h and 48h.

The qualitative assessment by TEM of internalization of CSNPs and nanomag®-D-spio revealed a rapid internalization of CSNPs of all three sizes in primary macrophages and dendritic cells after 2h. The intracellular localization of the particles

in endocytic vesicles directs towards an active uptake mechanism. In contrast, the internalization of nanomag®-D-spio in both cell types could be observed just after 24 h incubation time. The quantification of the uptake process by ICP-MS revealed significantly higher cellular internalization of CSNPs when compared to nanomag®-D-spio in human macrophages and dendritic cella, in a size and time dependent manner. The significant decrease in uptake of CSNPs after pretreatment of the cells with cytochalasin D provided an additional proof of an active internalization process involved.

To conclude, de novo synthesized silica coated CSNPS exhibited a cell type dependent toxicity with low cytotoxicity towards primary macrophages but with size, dose and time dependent toxicity in dendritic cells. Furthermore, involving an active process, and indicating a possible surface effect, silica-coated nanoparticles are internalized by a greater degree than the dextran coated nanoparticles in both cell types, in a time dependent manner.

4.3 PAPER III. COMPREHENSIVE ANALYSIS OF THE CORONA OF PALSMA PROTEINS ON SUPERPARAMAGNETIC IRON OXIDE NANOPARTICLES WITH DIFFERENT SURFACE COATINGS

The influence of the surface coating of SPION on the protein corona composition as well as on the cytotoxicity and uptake in human primary macrophages cultivated in the absence of fetal calf serum (FCS) was addressed in this work. Silica coated core shell nanoparticles with an overall size of ~ 50 nm and dextran coated nanomag®-D-spio with cluster size of 50 nm were used in this study.

The protein corona was formed upon *in vitro* incubation of the nanoparticles with pooled human plasma for 1 h, at 37°C. Centrifugation was used to separate the loosely bound “soft” corona from the “hard” corona attached on the surface of nanoparticles. The negative staining of the proteins revealed a nanoparticles’ surface dependent structural disposition of the protein corona: organized around the CSNPs and a diffuse appearance, visible as an organic layer on the whole micrographs in the case of nanomag®-D-spio.

Both CSNP and nanomag®-D-spio increased their hydrodynamic size after the addition of protein corona, although the mean hydrodynamic diameter of CSNPs - protein

corona increased 3-fold while the increase is not so significant for nanomag®-D-spio. The presence of the protein corona increases the zeta potential for the CSNP to -11,2 mV while for nanomag®-D-spio the value decreases to -9,8 mV.

The influence of the protein corona formation on the magnetic properties was investigated. For CSNPs - protein corona the r_2/r_1 values increase with 57 % at 20 MHz and 63 % at 60 MHz compared with CSNPs while for nanomag®-D-spio and nanomag®-D-spio - protein corona the values are increasing with maxim 1%.

The mitochondrial function of human primary macrophages was decreased in a time- and concentration-dependent manner upon exposure to CSNPs. In contrast, the mitochondrial function remains unaffected after exposure to CSNPs - protein corona, nanomag®-D-spio and nanomag®-D-spio - protein corona. Furthermore, no significant release of TNF – α was detected after incubation of the cells with the nanoparticles and nanoparticles – protein corona. The qualitative assessment of the internalization of the nanoparticles without and with protein corona could not visualize intracellular localization of nanomag®-D-spio and nanomag®-D-spio - protein corona particles whereas the CSNPs and CSNPs - protein corona are situated in membrane – enclosed vesicles.

Mass spectrometry performed on protein corona extracted from CSNPs and nanomag®-D-spio by on nanoparticle digestion showed a high reproducibility in protein identification with 72.8% (±2) overlap of identified proteins for nanomag®-D-spio and 71.9% (±5.7) for CSNPs from the no labeled analysis and calculated average standard deviations for the iTRAQ experiment of 14% for CSNP and 16% for nanomag®-D-spio.

The use of bioinformatics tools (statistical analysis, clustering analysis, Pathway and Gene Ontology (GO) enrichment analysis using Webgestalt tool and Ingenuity pathway analysis) revealed a high specificity of the protein corona to the surface of the nanoparticles. The extracted proteins were grouping in clusters that revealed an enrichment of the inflammatory proteins in the CSNPs corona and cell adhesion and tight junction related proteins in the nanomag®-D-spio corona.

Taken together, our data shows that the protein corona on the surface of the nanoparticles decreases the cytotoxicity (in the case of CSNPs) towards primary human

macrophages. Although by MS specific proteins are found to be enriched on the surface of the two different nanoparticles, no correlation between the presence of a particular protein in the protein corona and the observed biological effects can be identified at this stage and further investigation are thus warranted.

4.4 PAPER IV. SYNTHESIS, STURCTURAL AND MAGNETIC CHARACERISATION OF TRANSPARENT MAGNETIC IRON OXIDE/PMMA NANOCOMPOSITE

In this study, we report on the synthesis of homogeneous transparent FeOx/PMMA nanocomposites by in-situ polymerization. Magnetic and magneto-optical properties of the nanocomposites were investigated.

Oleic acid capped iron oxide nanoparticles with a mean diameter of ~ 26 nm and magnetite as dominant phase are obtained. The nanocomposite resulted is macroscopically slight brownish and transparent.

TGA and DSC analysis revealed that FeOx-PMMA nanocomposite with various iron oxide loading exhibit enhanced thermal stability compared to PMMA alone in the temperature range of 200–375 °C due to the presence of iron oxide nanoparticles.

The magnetic characterization of the composite by Angular Gradient Magnetometer showed an increase of the magnetization saturation/weight with the increase in the iron oxide loading with a remanence magnetization directly proportional to the inorganic nanoparticles loading. Furthermore, the Faraday rotation measurements showed the highest rotation of ca 0.5 deg/mm for the samples with the highest loading. As the rotation angle is proportional to the distance travelled by the light, a larger thickness of material with the same loading, or a higher loading of iron oxide nanoparticles, would be required for a substantial Faraday effect.

UV – Vis measurements were performed on the nanocomposites with different iron oxide loadings. The nanocomposites with a high loading of nanoparticles showed

absorption in the violet/blue region of the spectrum while lower loading nanocomposites have low absorption in the yellow/red.

To conclude, homogeneous transparent nanostructured materials were obtained and their physicochemical characterization was performed showing their magneto – optical possible applications such as for the fabrication of micro actuators, sensors, relays and magnetooptical devices.

5 DISCUSSION

Ideally, the design and the synthesis of a specific nanostructured material are pursued having a specific application as "target". The work presented in this thesis is an example of designing and preparing core – shell nanoparticles with defined characteristics and investigating in vitro all the possible implications of using their suspension as MRI contrast agent.

The necessity for synthesis of nanoparticles with well-controlled size and morphology is one of the basic requirements when advanced applications as in nanomedicine are desired. These applications also call for nanoparticles with more complex architecture such as core–shell structures that can carry several components with different functionality. Superparamagnetic iron oxide nanoparticles (SPION) are one of the most researched particles for applications in biology, medical diagnostics and therapy (178, 179). Surface-modified SPION are FDA approved materials for biological applications (180, 181). Silica is one of the preferred materials for coating the magnetic nanoparticles due to its high bio-stability, very low toxicity and versatile possibilities for surface functionalization via exposed silanol groups. In Paper I we developed a successful and reproducible fabrication route of finely tunable shell core – shell nanoparticle intended for magnetic visualizations applications. Understanding the synthesis mechanism was essential for a high reproducibility of the synthesis process. The formation of single iron oxide core - silica shell nanoparticles is the result of a controlled phase transfer of the cores in the water droplets of the dispersed phase and the subsequent homogeneous silica coating. Adjusting post synthesis the pH of the reaction in the region of minimum condensation of silica precursor and shock cooling the microemulsion resulted in highly separated particles, with no residual aggregation. The possibility that these nanoparticles might be used as MRI contrast agent are confirmed by the magnetic characteristics of the obtained nanoparticles such as superparamagnetism regardless of the silica thickness, high r2/r1 values compared to the commercial MRI contrast agents.

In order to promote a safe use of nanomaterials in biomedical applications, the nanoparticles interactions with the cells is important to address (182, 183). As macrophages and dendritic cells are important immune system components (184),

primary human monocyte derived macrophages (HMDM) and dendritic cells (MDDC) are more relevant in vitro model systems compared to the transformed cell lines. In paper II we studied the effect of SPIONs with different sizes on the primary human immune cells. The core shell nanoparticles synthesized using the method described in paper I (30 nm and 50 nm) and a combination of microemulsion method with silica condensation in water system (70 nm and 120 nm) were compared with cluster type, dextran coated SPIONs (nanomag®-D-spio) commercially available and similar to clinically used SPIONs. Dextran coated SPION exhibited very good biocompatibility in HMDM and HMDD, the viability of the immune cells being unaffected by the presence of nanomag®-D-spio in the cell culture media, as well as no release of proinflamatory citokines being observed. While no cytokine release was observed in HMDM and MDDC after exposure to CSNPs, a dose, time and cellular type dependent toxicity in primary human immunocompetent cells is observed. To discriminate between a true size dependent toxicity effect observed in HMDD and possible interferences with the remnant chemicals from the different synthesis process, particles with similar sizes with the 50 nm particles synthesized via inverse microemulsion method were synthesized in a similar way as the 120 nm particles. As no toxicity induced by possible remnant ethanol from the synthesis / post processing could be observed, a size dependent toxicity was concluded. However, other possible contaminants (in undetectable quantities but with toxic effect) from the synthesis cannot be excluded. Cellular internalization was investigated as the use as MRI contrast agent of SPION is one of the possible applications. The uptake (via an active process) seemed to be depending on the surface charge of the SPIONs as CSNPs were internalized to a much higher degree compared to nanomag®-D-spio. The observed differences in the hydrodynamic diameter of the nanoparticles dispersed in DI water and cell culture media as well as the surface dependent uptake contributed to the design of the following study (Paper III).

In paper III we questioned whether the corona of proteins formed on the surface of nanoparticles immediately after the nanoparticles enter in contact with biological fluids (136) has potential role in changing the magnetic properties and biological responses. For this study, we compared CSNPs with a diameter of approx. 50 nm and dextran coated nanomag®-D-spio with a cluster size of 50 nm. The incubation of the nanoparticles with pooled human plasma and the consequent washing process

allowed obtaining just the particles with a stable, "hard" corona, which were used for the subsequent experiments. Relevant for the use of these materials under in vivo conditions as MRI contrast agents, the magnetic properties and the contrasting properties (r2/r1 ratio) are measured. Alteration of the magnetic properties of the nanoparticles by the presence of the protein corona is observed. The modifications detected can be related to the presence of the protein corona and with the processing conditions for obtaining the nanoparticle-protein corona complexes. To assess the differences in toxicity of the nanoparticles without and with protein corona, the human primary macrophages were incubated in the absence of fetal calf serum. A dose - and time - dependent toxicity was seen for CSNPs without protein corona. A good biocompatibility was recorded though when cells were incubated with nanoparticle-corona complexes probably due to the presence of the protein corona and the decrease of the surface charge in the presence of the protein corona (185-187). The CSNPs non - toxicity in the presence of the protein corona is similar with the results in the paper II, where the fetal calf serum was the source of the proteins. The nanomag®-D-spio was similarly, non-cytotoxic, without or with protein corona. Cytokine measurements showed no significant release of TNF-α after incubation of the HMDM in the presence of silica or dextran coated SPIONs without or with protein corona, although effects on other cytokines or other soluble mediators cannot be excluded. Furthermore, the comprehensive analysis of the protein corona formed on the two types of particles using proteomics analysis was complemented by the use of bioinformatics tools. The analysis revealed a different distinct composition of the protein corona formed on the two types of particles, nanomag®-D-spio and CSNPs that might have possible very different implication in the biological responses. The protein corona extracted from the CSNPs surface is enriched in proteins implicated in complement, coagulation cascade and opsonisation as: complement components (3, 4A, 1q,9) and thrombin, coagulation factor XII, fibrinogen and apolipoproteins. These proteins are also important for opsonisation and subsequent uptake by the immune cells but also in systemic reactions as thrombosis and anaphylaxis (188, 189). This might correlate with the observed higher uptake of CSNPs – protein corona when compared to the nanomag®-D-spio – protein corona but also with the pristine CSNPs. Protein corona extracted from the nanomag®-D-spio surface is enriched in specific proteins different than the one obtained from the surface of CSNPs explained by the different surface charge. Enrichment of the cellular component cytoplasm and KEGG pathways focal cell adhesion and tight junction including integrins involved in caveolar mediated

endocytosis signaling may indicate that the nanomag®-D-spio protein corona is able to specifically interact with caveolae on the cell surface. We cannot conclude at this point in this work (and from the literature) if the observed interactions and effects on the cells are results of a specific component in biocorona or is a non specific effect (190).

In paper IV we synthesized 3D nanostructures in which iron oxide nanoparticles are dispersed in a PMMA matrix. The dispersed iron oxide nanoparticles are having a size of 26 nm above the superparamagnetic limit for iron oxide (around 15 nm) which is important when obtaining ferromagnetic composites is desired. Furthermore, the dispersed nanoparticles are having oleic acid as surface capping which renders their dispersibility in the monomers/oligomers during the in-site polymerization process (191) and close interaction with the organic phase. This is reflected from the TGA and DSC analysis that shows an enhanced thermal stability of the nanocomposites compared to the pure polymer probably due to the strong interfacial interactions between the polymer molecules and inorganic fillers. Due to the small size of inorganic nanoparticles and the homogeneous distribution of the nanoparticles in the polymer matrix, the nanocomposite has a good optical transparency proved by absorbance measurements. The UV-Vis spectroscopy on the composites showed characteristic UV-shielding properties of PMMA under 400 nm wavelength. The nanocomposites with high concentration of iron oxide absorb light in violet/blue region due to the strong absorbance of the nanoparticles in this region. When the distance between the nanoparticles decrease (correspondingly the concentration decreases) the absorbance shift towards yellow/red region of the spectrum that might render them applicable for magneto-optical application in this wavelength region.

6 CONCLUSIONS

In summary, the main results of this thesis are:

- Core shell nanoparticles with single iron oxide core and a finely tunable silica shell were synthesized via inverse microemulsion method. The prepared particles have a narrow size distribution, no aggregation retained and superparamagnetic character with sufficiently high magnetization, rendering them useful for biomedical applications, specifically as MRI T2 contrast agents.

- The core shell nanoparticles, exhibited a good biocompatibility when incubated *in vitro* with primary human immunocompetent cells. Furthermore, the cellular internalization of CSNPs by the human macrophages and dendritic cells is significantly higher compared to the internalization of the commercial dextran coated SPION, rendering them suitable for applications as MRI and cellular tracking.

- The coating of the SPION determined the formation of plasma protein coronas with distinct composition. Furthermore, the protein corona has an impact on the magnetic characteristics of the nanoparticles as well as on cell viability of human primary macrophages, effects more significantly observed for the CSNPs.

- 3D homogeneous transparent nanostructures with well dispersed iron oxide nanoparticles in the polymer matrix have been synthesis. The high bulk homogeneity and optical transparency, along with good magnetic properties makes them useful for magneto – optical applications.

Several nano-scale drug delivery systems eg. liposomal drug formulations of anti-cancer drugs and contrast agents for MRI based on nanoparticles are FDA approved today and already in use in clinics and many more are in different stages of development for targeting, diagnostic or therapeutic applications. Assessing the

interaction of nanomaterials with the biological systems is a key step in developing new nanomedicines (either new drugs nanoparticles based or imaging contrast agents) and evaluating their safety. Due to their specific properties (size, surface charge and surface molecules, shape, stability) nanoparticles have the capacity to cross biological barriers, to interact with the immune system, to be uptake intracellular and to affect the cellular functions. Furthermore, there is an emerging understanding in the literature that the observed effects of nanoparticles in nanomedicine are due to a combination between the intrinsic characteristics of the nanoparticles and the presence of an acquired corona of biomolecules in different biological media. Consequently, their essential properties that recommended them for certain applications (ex the ability to modify the relaxation rate of protons for MRI contrast agents) might be altered/changed by the adsorbed biocorona. This is particularly important for contrast agents with enhanced contrasting characteristics in vitro that might show different performances in the presence of biomolecules in vivo conditions.

In this thesis we combined the design and synthesis of nanoparticles for potential application as contrast agents in MRI with the assessment of the physical and chemical characteristics (size, surface charge, surface coating) and their magnetic characteristics. We investigated the influence of inherent characteristics of the nanoparticles on the interactions with immune cells as well as their in vitro biocompatibility in the absence/presence of proteins (fetal calf serum proteins and plasma). Modulation of their original magnetic properties was observed in the presence of the plasma protein corona. We conducted a comprehensive study of the composition of the protein corona and even if no correlation between the presence of a particular protein in the protein corona and the observed biological effects could be identified at this stage, further investigations are warranted. These studies contribute to the knowledge on the importance played by the biomolecules adsorbed on the surface of nanoparticles in triggering various responses in biological environment, in the incentive of developing better and safe nanoparticles for nanomedicine.

7 ACKNOWLEDGEMENTS

The period of my life that I will always call “PhD” has been a time of happiness and scientific development but also a time of sorrow and stress. Well, normal life one would say. I would not stand where I am now, a completely different person than the one that started the PhD few years back, without essential help from many persons in my life.

First of all I would like to thank my main supervisor Professor Bengt Fadeel. I am deeply grateful for the trust, patience and help you invested in me. With your scientific rectitude and enormous power to work you will always be my “scientific” model in life.

Muhammet Toprak, my co – supervisor. You have been always next to me and your positive thinking and extreme kindness helped me in conquering the fear that I will never manage. Thank you for being much more than a supervisor, being a friend!

Professor Sharon Stone – Elander, my mentor, thank you for kindly listening to my “ventilations” but also sharing your life experiences with me. It is always a pleasure to meet you!

I would like to thank to Professor Mamoun Muhammed, my supervisor from my “KTH” life for giving me the opportunity to enter in the fascinating “nano” world.

Professor Annika Scheynius thank you for organizing the NanoNet meetings (supported by Swedish Research Council), always scientifically enjoyable and a rare place of direct interaction between the “bio” and “materials” world.

Present and past members from KI: Andrea, Annette, Astrid, Erika, Jingwen, Consol, Fernando, Xiaoli, Giulio, Akihiro, Anda, Stefanie, Teresa, Rebecca, Sadollah, Hanna and Annika. Thank you for putting up with my direct stile, sharing your knowledge and nice lunch times with me.

Past and present members from KTH: Andrea, Sylvan and Peter thank you for your greatly cherished friendship! Sverker, Ying and Yang (Xiaodi), Abhilash, Robina, Fei, Salam, Mazher, Ramy, Mohsin, Mohsen, Terrance, Hans and Wubeshet, Nader, Yichen, Adrineh, Milad, Najmeh you made the working life much more pleasant!

The work performed during my PhD studies was supported in part by grants from FP7 programs (INNOMED; NANNOMUNE, BIODIAGNOSTIC), FORMAS, FAS and Karolinska Institutet.

My coauthors and collaborators: Sophie Laurent, Jean-Luc Bridot and Robert N. Muller, Andrea Kunzmann, Britta Andersson, Susanne Gabrielsson, Tina Buerki-Thurnherr, Marie Vahter, Harald Krug, Maria Pernemalm, Janne Lehtiö, Pekka

Kohonen, Roland Grafström, Sergiy Khartsev, Alexander Grishin, Kjell Hultenby thank you for the fruitful collaborations and giving me the opportunity to learn from you.

To my dear friend Neus, thank you for being with me all these times! I treasure your friendship!

To my friends Anna and Per, thank you for being our family here when life was unexpectedly painful for us. We will never forget your help!

To my mam and dad, and my sister Oana thank you for being always there for me! Without your love and support I would never be the person I am today. To my mama Ursula and tata Dieter, sister Conny and brother Markus thank you for your loving patience and accepting me the way I am.

To the love of my life and my best friend Uli, thank you for being unconditionally always next to me. You earned this PhD as much as me! Johannes and Lucas, the most precious children in the world, thank you for always reminding me that there is real life beyond my PhD!

8 REFERENCES

1. Buzea C, Blandino IIP, Robbie K. Nanomaterials and nanoparticles: Sources and toxicity. Biointerphases. 2007;2(4):MR17 - MR1721.
2. Oberdörster G, Oberdörster E, Oberdörster J. Nanotoxicology: An Emerging Discipline Evolving from Studies of Ultrafine Particles. Environ Health Perspect. 2005;113(7).
3. Nyström AM, Fadeel B. Safety assessment of nanomaterials: Implications for nanomedicine. Journal of Controlled Release. (0).
4. Gleiter H. Nanostructured materials: state of the art and perspectives. Nanostructured Materials. 1995;6(1–4):3-14.
5. Pokropivny VV, Skorokhod VV. Classification of nanostructures by dimensionality and concept of surface forms engineering in nanomaterial science. Materials Science and Engineering: C. 2007;27(5–8):990-3.
6. Arora S, Rajwade JM, Paknikar KM. Nanotoxicology and in vitro studies: The need of the hour. Toxicology and Applied Pharmacology. 2012;258(2):151-65.
7. Nel A, Xia T, Mädler L, Li N. Toxic Potential of Materials at the Nanolevel. Science. 2006 February 3, 2006;311(5761):622-7.
8. Laurent S, Forge D, Port M, Roch A, Robic C, Vander Elst L, et al. Magnetic iron oxide nanoparticles: synthesis, stabilization, vectorization, physicochemical characterizations and biological applications. Chemical reviews. 2008;108:2064-110.
9. Pecharromfin C, Gonzfilez-Carrefio T, Iglesias JE. The infrared dielectric properties of maghemite, γ-Fe_2O_3, from reflectance measurement on pressed powders. Physics and Chemistry of Minerals. 1995;22:21-9.
10. Morales MP, Bomati-Miguel O, Perez de Alejo R, Ruiz-Cabello J, Veintemillas-Verdaguer S, O'Grady K. Contrast agents for MRI based on iron oxide nanoparticles prepared by laser pyrolysis. Journal of Magnetism and Magnetic Materials. 2003;266:102-9.
11. Julian-Lopez B, Boissiere C, Chaneac C, Grosso D, Vasseur S, Miraux S, et al. Mesoporous maghemite–organosilica microspheres: a promising route towards multifunctional platforms for smart diagnosis and therapy. Journal of Materials Chemistry. 2007;17:1563-9.
12. Pascal C, Pascal JL, Favier F, Elidrissi Moubtassim ML, Payen C. Electrochemical synthesis for the control of γ-Fe_2O_3 nanoparticle size, morphology, microstructure and magnetic behavior. Chemistry of Materials. 1999;11:141-7.
13. Khan HR, Petrikowski K. Anisotropic structural and magnetic properties of arrays of $Fe_{26}Ni_{74}$ nanowires electrodeposited in the pores of anodic alumina. Journal of Magnetism and Magnetic Materials. 2000;215-216:526-8.
14. Salazar-Alvarez G, Muhammed M, Zagorodni AA. Novel flow injection synthesis of iron oxide nanoparticles with narrow size distribution. Chemical Engineering Science. 2006;61:4625 - 33.
15. Massart R. Preparation of aqueous magnetic liquids in alkaline and acidic media. IEEE Transactions on Magnetics. 1981;MAG-17:1247-8.
16. Jolivet J-P, Chanéac C, Tronc E. Iron oxide chemistry. From molecular clusters to extended solid networks. Chemical Communications. 2004;5:481-7.
17. Babes L, Denizot B, Tanguy G, Le Jeune JJ, Jallet P. Synthesis of iron oxide nanoparticles used as MRI contrast agents: a parametric study. Journal of Colloid and Interface Science. 1999;212:474-82.
18. Lu A-H, Salabas EL, Schuth F. Magnetic nanoparticles: synthesis, protection, functionalization and application. Angewandte Chemie International Edition. 2007;46:1222 - 44.
19. Teja AS, Koh P-Y. Synthesis, properties and applications of magnetic iron oxide nanoparticles. Progress in Crystal Growth and Characterization of Materials. 2009;55:22-45.

20. Lopez-Quintela MA, Tojob C, Blanco MC, Garcıa Rio L, Leis JR. Microemulsion dynamics and reactions in microemulsions. Current Opinion in Colloid and Interface Science. 2004;9:264-78.
21. Capek I. Preparation of metal nanoparticles in water-in-oil (w/o) microemulsions. Advances in Colloid and Interface Science. 2004;110:49-74.
22. Munshi N, De TK, Maitra A. Size modulation of polymeric nanoparticles under controlled dynamics of microemulsion droplets. Journal of Colloid and Interface Science. 1997;190:387-91.
23. Pileni M-P. The role of soft colloidal templates in controlling the size and shape of inorganic nanocrystals. Nature Materials. 2003;2:145-50.
24. Sue K, Kimura K, Arai K. Hydrothermal synthesis of ZnO nanocrystals using microreactor. Materials Letters. 2004;58:3229- 31.
25. Chen D, Xu R. Hydrothermal synthesis and characterization of nanocrystalline Fe_3O_4 powders. Materials Research Bulletin. 1998;33:1015-21.
26. Fievet F, Lagier JP, Blin B, Beaudoin B, Figlarz M. Homogeneous and heterogeneous nucleations in the polyol process for the preparation of micron and submicron size metal particles. Solid State Ionics. 1989;32-33:198-205.
27. Jezequel D, Guenot J, Jouini N, Fievet F. Submicrometer zinc oxide particles: elaboration in polyol medium and morphological characteristics. Journal of Materials Research. 1995;10:77-83.
28. Rockenberger J, Scher EC, Alivisatos AP. A new nonhydrolytic single-precursor approach to surfactant-capped nanocrystals of transition metal oxides. Journal of American Chemical Society. 1999;121:11595-6.
29. Hyeon T, Lee SS, Park J, Chung Y, Bin Na H. Synthesis of highly crystalline and monodisperse maghemite nanocrystallites without a size-selection process. Journal of American Chemical Society. 2001;123:12798-801.
30. Sun S, Zeng H, Robinson DB, Raoux S, Rice PM, Wang SX, et al. Monodisperse MFe_2O_4 (M = Fe, Co, Mn) nanoparticles. Journal of American Chemical Society. 2004;126 273-9.
31. Park J, An K, Hwang Y, Park J-G, Noh H-J, Kim J-Y, et al. Ultra-large-scale syntheses of monodisperse nanocrystals. Nature Materials. 2004;3:891-5.
32. Jana NR, Chen Y, Peng X. Size - and shape - controlled magnetic (Cr, Mn, Fe, Co, Ni) oxide nanocrystals via a simple and general approach. Chemistry of Materials. 2004;16:3931-5.
33. Yu WW, Falkner JC, Yavuz CT, Colvin VL. Synthesis of monodisperse iron oxide nanocrystals by thermal decomposition of iron carboxylate salts. Chemical Communications. 2004:2306-7.
34. Lin C-R, Chiang R-K, Wang J-S, Sung T-W. Magnetic properties of monodisperse iron oxide nanoparticles. Journal of Applied Physics. 2006; 99:08N710.
35. Stoeber W, Fink A, Bohn E. Controlled growth of monodisperse silica spheres in the micron size range. Journal of Colloid and Interface Science. 1968;26:62-9.
36. Im SH, Herricks T, Lee YT, Xia Y. Synthesis and characterization of monodisperse silica colloids loaded with superparamagnetic iron oxide nanoparticles. Chemical Physics Letters. 2005;401:19-23.
37. Lu Y, Yin Y, Mayers BT, Xia Y. Modifying the surface properties of superparamagnetic iron oxide nanoparticles through a sol-gel approach. Nano Letters. 2002;2:183-6.
38. Deng Y-H, Wang C-C, Hu J-H, Yang W-L, Fu S-K. Investigation of formation of silica -coated magnetite nanoparticles via sol-gel approach. Colloids and Surfaces, A: Physicochemical and Engineering Aspects. 2005;262:87-93.
39. Barnakov YA, Yu MH, Rosenzweig Z. Manipulation of the magnetic properties of magnetite - silica nanocomposite materials by controlled Stober synthesis. Langmuir. 2005;21:7524-7.
40. Sharma P, Brown S, Walter G, Santra S, Moudgil B. Nanoparticles for bioimaging. Advances in Colloid and Interface Science. 2006;123-126:471-85.
41. Lu C-W, Hung Y, Hsiao J-K, Yao M, Chung T-H, Lin Y-S, et al. Bifunctional magnetic silica nanoparticles for highly efficient human stem cell labeling. Nano letters. 2007;7:149-54.

42. Liu H-M, Wu S-H, Lu C-W, Yao M, Hsiao J-K, Hung Y, et al. Mesoporous silica nanoparticles improve magnetic labeling efficiency in human stem cells. Small. 2008;4:619-26.
43. Osseo-Asare K, Arriagada FJ. Preparation of silica nanoparticles in a non-ionic reverse micellar system. Colloids and Surfaces. 1990;50:321-39.
44. Arriagada FJ, Osseo-Asare K. Phase and dispersion stability effects in the synthesis of silica nanoparticles in a non-ionic reverse microemulsion. Colloids and Surfaces. 1992;69:105-15.
45. Arriagada FJ, Osseo-Asare K. Synthesis of nanosize silica in a nonionic water-in-oil microemulsion: effects of the water/surfactant molar ratio and ammonia concentration. Journal of Colloid and Interface Science. 1999;211:210-20.
46. Arriagada FJ, Osseo-Asare K. Controlled hydrolysis of tetraethoxysilane in a nonionic water-in-oil microemulsion: a statistical model of silica nucleation. Colloids and Surfaces, A: Physicochemical and Engineering Aspects. 1999;154:311-26.
47. Osseo-Asare K, Arriagada FJ. Growth Kinetics of Nanosize Silica in a Nonionic Water-in-Oil Microemulsion: A Reverse Micellar Pseudophase Reaction Model. Journal of Colloid and Interface Science. 1999;218:68-76.
48. Lu C-W, Hung Y, Hsiao J-K, Yao M, Chung T-H, Lin Y-S, et al. Bifunctional magnetic silica nanoparticles for highly efficient human stem cell labelling. Nano Letters. 2007;7:149-54.
49. Yi DK, Lee SS, Papaefthymiou GC, Ying JY. Nanoparticle architectures templated by SiO_2/Fe_2O_3 nanocomposites. Chemistry of Materials. 2006;18:614-9.
50. Zhang M, Cushing BL, O'Connor CJ. Synthesis and characterization of monodisperse ultra-thin silica-coated magnetic nanoparticles. Nanotechnology. 2008;19:085601/1-/5.
51. Yi DK, Selvan ST, Lee SS, Papaefthymiou GC, Kundaliya D, Ying JY. Silica-coated nanocomposites of magnetic nanoparticles and quantum dots. Journal of American Chemical Society. 2005;127:4990-1.
52. Narita A, Nakab K, Chujo Y. Facile control of silica shell layer thickness on hydrophilic iron oxide nanoparticles via reverse micelle method. Colloids and Surfaces A: Physicochemical and Engineering Aspects. 2009;336:46–56.
53. Cheng J, Teply BA, Sherifi I, Sung J, Luther G, Gu FX, et al. Formulation of functionalized PLGA–PEG nanoparticles for in vivo targeted drug delivery. Biomaterials. 2007;28:869-76.
54. Kim BYS, Rutka JT, Chan WCW. Nanomedicine. New England Journal of Medicine. 2010;363(25):2434-43.
55. Bean CP, Livingston JD. Superparamagnetism. Journal of Applied Physics. 1959;30:S120-S9.
56. Li S, Lin MM, Toprak MS, Kim DK, Muhammed M. Nanocomposites of polymer and inorganic nanoparticles for optical and magnetic applications2010.
57. Wilson JL, Poddar P, Frey NA, Srikanth H, Mohomed K, Harmon JP, et al. Synthesis and magnetic properties of polymer nanocomposites with embedded iron nanoparticles. Journal of Applied Physics. 2004;95:1439.
58. Fang J, Tung LD, Stokes KL, He J, Caruntu D, Zhou WL, et al. Synthesis and magnetic properties of CoPt–poly(methylmethacrylate) nanostructured composite material. Journal of Applied Physics 2002;91(10):8816-19.
59. Gass J, Poddar P, Almand J, Srinath S, Srikanth H. Superparamagnetic Polymer Nanocomposites with Uniform Fe3O4 Nanoparticle Dispersions. Advanced Functional Materials. 2006;16(1):71-5.
60. Prabhakaran T, Hemalatha J. Synthesis and characterization of magnetoelectric polymer nanocomposites. Journal of Polymer Science Part B: Polymer Physics. 2008;46(22):2418-22.
61. Guo Z, Lei K, Li Y, Ng HW, Prikhodko S, Hahn HT, et al. Fabrication and characterization of iron oxide nanoparticles reinforced vinyl-ester resin nanocomposites. Composites Science and Technology. 2008;68:1513-20.
62. Gach PC, Sims CE, Allbritton NL. Transparent magnetic photoresists for bioanalytical applications. Biomaterials. 2010;31(33):8810-7.
63. Weissleder R. Scaling down imaging: molecular mapping of cancer in mice. Nature Reviews Cancer. 2002;2:1-8.

64. Berry CC, Curtis ASG. Functionalisation of magnetic nanoparticles for applications in biomedicine. Journal of Physics D: Applied Physics. 2003;36:R198-R206.
65. McRobbie DW, Moore EA, Graves MJ, Prince MR. MRI from picture to proton. Cambridge: Cambridge University Press; 2007.
66. Bowtell R. Medical imaging: Colourful future for MRI. Nature. 2008;453:993 - 4.
67. Lok C. Picture perfect. Nature. 2001;412:372-5.
68. Rinck PA, Jones RA, Kvaerness J, Southon TE, De Francisco P, Muller RN, et al. Magnetic resonance in medicine. Oxford: Blackwell Scientific Publications; 1993.
69. Yan G-P, Robinson L, Hogg P. Magnetic resonance imaging contrast agents: overview and perspectives. Radiography. 2007;13:e5-e19.
70. Taylor KML, Kim JS, Rieter WJ, An H, Lin W, Lin W. Mesoporous Silica Nanospheres as Highly Efficient MRI Contrast Agents. Journal of the American Chemical Society. 2008 2008/02/01;130(7):2154-5.
71. Hartman KB, Laus S, Bolskar RD, Muthupillai R, Helm L, Toth E, et al. Gadonanotubes as Ultrasensitive pH-Smart Probes for Magnetic Resonance Imaging. Nano Letters. 2008 2008/02/01;8(2):415-9.
72. Kim J, Kim HS, Lee N, Kim T, Kim H, Yu T, et al. Multifunctional Uniform Nanoparticles Composed of a Magnetite Nanocrystal Core and a Mesoporous Silica Shell for Magnetic Resonance and Fluorescence Imaging and for Drug Delivery. Angewandte Chemie International Edition. 2008;47(44):8438-41.
73. Sun C, Lee JSH, Zhang M. Magnetic nanoparticles in MR imaging and drug delivery. Advanced Drug Delivery Reviews. 2008;60: 1252-65.
74. McCarthy JR, Weissleder R. Multifunctional magnetic nanoparticles for targeted imaging and therapy. Advanced Drug Delivery Reviews. 2008;60:1241-51.
75. Lawaczeck R, Menzel M, Pietsch H. Superparamagnetic iron oxide particles: contrast media for magnetic resonance imaging. Applied Organometallic Chemistry. 2004;18:506-13.
76. Kohler N, Sun C, Wang J, Zhang M. Methotrexate-modified superparamagnetic nanoparticles and their intracellular uptake into human cancer cells. Langmuir. 2005;21:8858-64.
77. Zweers MLT, Engbers GHM, Grijpma DW, Feijen J. In vitro degradation of nanoparticles prepared from polymers based on dl-lactide, glycolide and poly(ethylene oxide). Journal of Controlled Release. 2004;100:347-56.
78. Leo E, Brina B, Forni F, Vandelli MA. In vitro evaluation of PLA nanoparticles containing a lipophilic drug in water-soluble or insoluble form. International Journal of Pharmaceutics. 2004;278:133-41.
79. Shenoy DB, Amiji MM. Poly(ethylene oxide)-modified poly(ε-caprolactone) nanoparticles for targeted delivery of tamoxifen in breast cancer. International Journal of Pharmaceutics. 2005;293:261-70.
80. Muller RH, Keck CM. Challenges and solutions for the delivery of biotech drugs – a review of drug nanocrystal technology and lipid nanoparticles. Journal of Biotechnology. 2004;113:151-70.
81. Yang SC, Lu LF, Cai Y, Zhu JB, Liang BW, Yang CZ. Body distribution in mice of intravenously injected camptothecin solid lipid nanoparticles and targeting effect on brain. Journal of Controlled Release. 1999;59: 299-307.
82. Zara GP, Cavalli R, Bargoni A, Fundaro A, Vighetto D, Gasco MR. Intravenous Administration to Rabbits of Non-stealth and Stealth Doxorubicin-loaded Solid Lipid Nanoparticles at Increasing Concentrations of Stealth Agent: Pharmacokinetics and Distribution of Doxorubicin in Brain and Other Tissues. Journal of Drug Targeting. 2002;10:327-35.
83. Roy I, Ohulchanskyy TY, Pudavar HE, Bergey EJ, Oseroff AR, Morgan J, et al. Ceramic-Based Nanoparticles Entrapping Water-Insoluble Photosensitizing Anticancer Drugs: A Novel Drug−Carrier System for Photodynamic Therapy. J Am Chem Soc. 2003;125:7860-5.
84. Chen J-F, Ding H-M, Wang J-X, Shao L. Preparation and characterization of porous hollow silica nanoparticles for drug delivery application. Biomaterials. 2004;25:723-7.

85. Bhakta G, Mitra S, Maitra A. DNA encapsulated magnesium and manganous phosphate nanoparticles: potential non-viral vectors for gene delivery. Biomaterials. 2005;26 2157-63.
86. Uhrich KE, Cannizzaro SM, Langer RS, Shakesheff KM. Polymeric Systems for Controlled Drug Release. Chem Rev. 1999;99:3181-98.
87. Vinogradov SV, Batrakova EV, Kabanov AV. Nanogels for Oligonucleotide Delivery to the Brain. Bioconjugate Chem. 2004;15:50-60.
88. McAllister KP, Sazani M, Adam M, Cho J, Rubinstein M, Samulski RJ, et al. Polymeric Nanogels Produced via Inverse Microemulsion Polymerization as Potential Gene and Antisense Delivery Agents. J Am Chem Soc. 2002;124 15198-207.
89. Bajpai AK, Shukla SK, Bhanu S, Kankane S. Responsive polymers in controlled drug delivery. Progress in Polymer Science. 2008;33:1088-118.
90. Becerra-Bracamontes F, Sanchez-Diaz JC, Gonzalez-Alvarez A, Ortega-Gudino P, Michel-Valdivia E, Martinez-Ruvalcaba A. Design of a Drug Delivery System Based on Poly(acrylamide-co-acrylic acid)/Chitosan Nanostructured Hydrogels. Journal of Applied Polymer Science. 2007;106:3939-44.
91. Kost J, Langer R. Responsive polymeric delivery systems. Advanced Drug Delivery Reviews. 2001;46:125-48.
92. McCarthy JR, Jaffer FA, Weissleder R. A Macrophage-Targeted Theranostic Nanoparticle for Biomedical Applications. Small. 2006;2(8-9):983-7.
93. Larson TA, Bankson J, Aaron J, Sokolov K. Hybrid plasmonic magnetic nanoparticles as molecular specific agents for MRI/optical imaging and photothermal therapy of cancer cells. Nanotechnology. 2007;18(32):325101.
94. Oberdörster G. Safety assessment for nanotechnology and nanomedicine: concepts of nanotoxicology. Journal of Internal Medicine. 2010;267(1):89-105.
95. The dose makes the poison. Nature Nanotechnology. 2011;6(6):329-.
96. Donaldson K, Stone V, Tran CL, Kreyling W, Borm PJA. Nanotoxicology. Occupational and Environmental Medicine. 2004 September 1, 2004;61(9):727-8.
97. Maynard AD, Warheit DB, Philbert MA. The New Toxicology of Sophisticated Materials: Nanotoxicology and Beyond. Toxicological Sciences. 2011 March 1, 2011;120(suppl 1):S109-S29.
98. Krug HF, Wick P. Nanotoxicology: An Interdisciplinary Challenge. Angewandte Chemie International Edition. 2011;50(6):1260-78.
99. Clift MJD, Blank F, Gehr P, Rothen-Rutishauser B. Nanotoxicology: A Brief Overview and Discussion of the Current Toxicological Testing In Vitro and Suggestions for Future Research. General, Applied and Systems Toxicology: John Wiley & Sons, Ltd; 2009.
100. Oberdörster G, Ferin J, Morrow PE. Volumetric Loading of Alveolar Macrophages (AM): A Possible Basis for Diminished AM-Mediated Particle Clearance. Experimental Lung Research. 1992;18(1):87-104.
101. Oberdörster G, Sharp Z, Atudorei V, Elder A, Gelein R, Kreyling W, et al. Translocation of Inhaled Ultrafine Particles to the Brain. Inhalation Toxicology. 2004;16(6-7):437-45.
102. Maynard AD, Aitken RJ, Butz T, Colvin V, Donaldson K, Oberdorster G, et al. Safe handling of nanotechnology. Nature. 2006;444(7117):267-9.
103. Ryman-Rasmussen JP, Cesta MF, Brody AR, Shipley-Phillips JK, Everitt JI, Tewksbury EW, et al. Inhaled carbon nanotubes reach the subpleural tissue in mice. Nature Nanotechnology. 2009;4(11):747-51.
104. Pauluhn J. Subchronic 13-Week Inhalation Exposure of Rats to Multiwalled Carbon Nanotubes: Toxic Effects Are Determined by Density of Agglomerate Structures, Not Fibrillar Structures. Toxicological Sciences. 2010 January 1, 2010;113(1):226-42.
105. Kagan VE, Konduru NV, Feng W, Allen BL, Conroy J, Volkov Y, et al. Carbon nanotubes degraded by neutrophil myeloperoxidase induce less pulmonary inflammation. Nature Nanotechnology. 2010;5(5):354-9.
106. Ryman-Rasmussen JP, Riviere JE, Monteiro-Riviere NA. Penetration of Intact Skin by Quantum Dots with Diverse Physicochemical Properties. Toxicological Sciences. 2006 May 2006;91(1):159-65.

107. Choksi AN, Poonawalla T, Wilkerson MG. Nanoparticles: a closer look at their dermal effects. J Drugs Dermatol. 2010;9(5):475-81.
108. Hansen SF, Michelson ES, Kamper A, Borling P, Stuer-Lauridsen F, Baun A. Categorization framework to aid exposure assessment of nanomaterials in consumer products. Ecotoxicology. 2008;17(5):438-47.
109. Mahler GJ, Esch MB, Tako E, Southard TL, Archer SD, Glahn RP, et al. Oral exposure to polystyrene nanoparticles affects iron absorption. Nature Nanotechnology. 2012;7(4):264-71.
110. Dranoff G. Cytokines in cancer pathogenesis and cancer therapy. Nat Rev Cancer. 2004;4(1):11-22.
111. Dobrovolskaia MA, Patri AK, Zheng J, Clogston JD, Ayub N, Aggarwal P, et al. Interaction of colloidal gold nanoparticles with human blood: effects on particle size and analysis of plasma protein binding profiles. Nanomedicine : nanotechnology, biology, and medicine. 2009;5(2):106-17.
112. Balakrishnan B, Kumar DS, Yoshida Y, Jayakrishnan A. Chemical modification of poly(vinyl chloride) resin using poly(ethylene glycol) to improve blood compatibility. Biomaterials. 2005;26(17):3495-502.
113. Moghimi SM, Andersen AJ, Ahmadvand D, Wibroe PP, Andresen TL, Hunter AC. Material properties in complement activation. Advanced Drug Delivery Reviews. 2011;63(12):1000-7.
114. Moghimi SM, Hunter AC, Dadswell CM, Savay S, Alving CR, Szebeni J. Causative factors behind poloxamer 188 (Pluronic F68, Flocor™)-induced complement activation in human sera: A protective role against poloxamer-mediated complement activation by elevated serum lipoprotein levels. Biochimica et Biophysica Acta (BBA) - Molecular Basis of Disease. 2004;1689(2):103-13.
115. Gbadamosi JK, Hunter AC, Moghimi SM. PEGylation of microspheres generates a heterogeneous population of particles with differential surface characteristics and biological performance. FEBS Letters. 2002;532(3):338-44.
116. Bertholon I, Vauthier C, Labarre D. Complement Activation by Core–Shell Poly(isobutylcyanoacrylate)–Polysaccharide Nanoparticles: Influences of Surface Morphology, Length, and Type of Polysaccharide. Pharmaceutical Research. 2006;23(6):1313-23.
117. Dobrovolskaia MA, McNeil SE. Immunological properties of engineered nanomaterials. Nature Nanotechnology. 2007;2:469 - 78.
118. Mottram PL, Leong D, Crimeen-Irwin B, Gloster S, Xiang SD, Meanger J, et al. Type 1 and 2 Immunity Following Vaccination Is Influenced by Nanoparticle Size: Formulation of a Model Vaccine for Respiratory Syncytial Virus. Molecular Pharmaceutics. 2006 2007/02/01;4(1):73-84.
119. Moyano DF, Goldsmith M, Solfiell DJ, Landesman-Milo D, Miranda OR, Peer D, et al. Nanoparticle Hydrophobicity Dictates Immune Response. Journal of the American Chemical Society. 2012 2012/03/07;134(9):3965-7.
120. Tan Y, Li S, Pitt BR, Huang L. The Inhibitory Role of CpG Immunostimulatory Motifs in Cationic Lipid Vector-Mediated Transgene Expression in Vivo. Human Gene Therapy. 2004;10(13):2153-61.
121. Stieneker F, Kreuter J, Lower J. High antibody titres in mice with polymethylmethacrylate nanoparticles as adjuvant for HIV vaccines. AIDS (London, England). 1991;5(4):431-5.
122. Castignolles N, Morgeaux S, Gontier-Jallet C, Samain D, Betbeder D, Perrin P. A new family of carriers (biovectors) enhances the immunogenicity of rabies antigens. Vaccine. 1996;14(14):1353-60.
123. Walkey CD, Chan WCW. Understanding and controlling the interaction of nanomaterials with proteins in a physiological environment. Chemical Society Reviews. 2012.
124. Walczyk D, Baldelli Bombelli F, Monopoli MP, Lynch I, Dawson KA. What the Cell "Sees" in Bionanoscience. Journal of the American Chemical Society. 2010;132:5761-8.
125. Hellstrand E, Lynch I, Andersson A, Drakenberg T, Dahlbäck B, Dawson KA, et al. Complete high-density lipoproteins in nanoparticle corona. FEBS Journal. 2009;276(12):3372-81.

126. Nel AE, Mädler L, Velegol D, Xia T, Hoek EMV, Somasundaran P, et al. Understanding biophysicochemical interactions at the nano–bio interface. Nature Materials. 2009;8:543-57.
127. Walkey CD, Olsen JB, Guo H, Emili A, Chan WCW. Nanoparticle Size and Surface Chemistry Determine Serum Protein Adsorption and Macrophage Uptake. Journal of the American Chemical Society. 2011 2012/02/01;134(4):2139-47.
128. Vroman L. Effect of Adsorbed Proteins on the Wettability of Hydrophilic and Hydrophobic Solids. Nature. 1962;196(4853):476-7.
129. Vroman L, Adams AL. Identification of rapid changes at plasma–solid interfaces. Journal of Biomedical Materials Research. 1969;3(1):43-67.
130. Vroman L, Adams A, Fischer G, Munoz P. Interaction of high molecular weight kininogen, factor XII, and fibrinogen in plasma at interfaces. Blood. 1980 January 1, 1980;55(1):156-9.
131. Dell'Orco D, Lundqvist M, Oslakovic C, Cedervall T, Linse S. Modeling the Time Evolution of the Nanoparticle-Protein Corona in a Body Fluid. PLoS ONE. 2010;5(6):e10949.
132. Casals E, Pfaller T, Duschl A, Janneke Oostingh G, Puntes V. Time evolution of the nanoparticle protein corona. ACS Nano. 2010;4(7):3623–32.
133. Casals E, Pfaller T, Duschl A, Oostingh GJ, Puntes VF. Hardening of the Nanoparticle–Protein Corona in Metal (Au, Ag) and Oxide (Fe3O4, CoO, and CeO2) Nanoparticles. Small. 2011;7(24):3479-86.
134. Cedervall T, Lynch I, Lindman S, Berggård T, Thulin E, Nilsson H, et al. Understanding the nanoparticle–protein corona using methods to quantify exchange rates and affinities of proteins for nanoparticles. Proceedings of National Academy of Sciences of the United States of America. 2007;104 (7):2050–5.
135. Milani S, Baldelli Bombelli F, Pitek AS, Dawson KA, Radler J. Reversible Versus Irreversible Binding of Transferrin to Polystyrene Nanoparticles: Soft and Hard Corona. ACS Nano. 2012.
136. Jansch M, Stumpf P, Graf C, Rühl E, Müller RH. Adsorption kinetics of plasma proteins on ultrasmall superparamagnetic iron oxide (USPIO) nanoparticles. International Journal of Pharmaceutics. 2012;428(1–2):125-33.
137. Lundqvist M, Stigler J, Cedervall T, Berggård T, Flanagan MB, Lynch I, et al. The evolution of the protein corona around nanoparticles: a test study. ACS Nano. 2011.
138. Klein J. Probing the interactions of proteins and nanoparticles. Proceedings of National Academy of Sciences of the United States of America. 2007;104(7):2029-30.
139. Tenzer S, Docter D, Rosfa S, Wlodarski A, Kuharev J, Rekik A, et al. Nanoparticle Size Is a Critical Physicochemical Determinant of the Human Blood Plasma Corona: A Comprehensive Quantitative Proteomic Analysis. ACS Nano. 2011 2011/09/27;5(9):7155-67.
140. Cho W-S, Duffin R, Thielbeer F, Bradley M, Megson IL, MacNee W, et al. Zeta Potential and Solubility to Toxic Ions as Mechanisms of Lung Inflammation Caused by Metal/Metal Oxide Nanoparticles. Toxicological Sciences. 2012 April 1, 2012;126(2):469-77.
141. Lundqvist M, Stigler J, Elia G, Lynch I, Cedervall T, Dawson KA. Nanoparticle size and surface properties determine the protein corona with possible implications for biological impacts. Proceedings of National Academy of Sciences of the United States of America 2008;105(38):14265–70.
142. Devine DV, Wong K, Serrano K, Chonn A, Cullis PR. Liposome—complement interactions in rat serum: implications for liposome survival studies. Biochimica et Biophysica Acta (BBA) - Biomembranes. 1994;1191(1):43-51.
143. Cedervall T, Lynch I, Foy M, Berggård T, Donnelly SC, Cagney G, et al. Detailed identification of plasma proteins adsorbed on copolymer nanoparticles. Angewandte Chemie International Edition. 2007;46:5754 -6.
144. Alhareth K, Vauthier C, Bourasset F, Gueutin C, Ponchel G, Moussa F. Conformation of surface-decorating dextran chains affects the pharmacokinetics and biodistribution of doxorubicin-loaded nanoparticles. European Journal of Pharmaceutics and Biopharmaceutics. (0).

145. Derfus AM, Chan WCW, Bhatia SN. Probing the Cytotoxicity of Semiconductor Quantum Dots. Nano Letters. 2003 2004/01/01;4(1):11-8.
146. Gurr J-R, Wang ASS, Chen C-H, Jan K-Y. Ultrafine titanium dioxide particles in the absence of photoactivation can induce oxidative damage to human bronchial epithelial cells. Toxicology. 2005;213(1–2):66-73.
147. Stöber W, Fink A. Controlled Growth of Monodisperse Silica Spheres in the Micron Size Range. Journal of colloid and interface science. 1968;26:62--9.
148. Sih BC, Wolf MO. Metal nanoparticle-conjugated polymer nanocomposites. Chemical Communications. 2005(27):3375-84.
149. Lopez-Santiago A, Gangopadhyay P, Thomas J, Norwood RA, Persoons A, Peyghambarian N. Faraday rotation in magnetite-polymethylmethacrylate core-shell nanocomposites with high optical quality. Applied Physics Letters 2009; 95:143302.
150. Corot C, Robert P, Idée J-M, Port M. Recent advances in iron oxide nanocrystal technology for medical imaging. Advanced Drug Delivery Reviews. 2006;58:1471-504.
151. Graham CD. High-Sensitivity Magnetization Measurements. Journal of Materials Science and Technology. 2000;16(2):97-101.
152. Taboada E, del Real RP, Gich M, Roig A, Molins E. Faraday rotation measurements in maghemite-silica aerogels. Journal of Magnetism and Magnetic Materials. 2006;301(1):175-80.
153. Romani N, Reider D, Heuer M, Ebner S, Kämpgen E, Eibl B, et al. Generation of mature dendritic cells from human blood An improved method with special regard to clinical applicability. Journal of Immunological Methods. 1996;196(2):137-51.
154. Tedder TF, Jansen PJ. Isolation and Generation of Human Dendritic Cells. Current Protocols in Immunology. 1997;Unit 7.32: 7.32.1-7..16.
155. Davies JQ, Gordon S. Isolation and Culture of Human Macrophages. Methods in Molecular Biology. 2005;290:105-16.
156. Khazen W, M'Bika J-P, Tomkiewicz C, Benelli C, Chany C, Achour A, et al. Expression of macrophage-selective markers in human and rodent adipocytes. FEBS Letters. 2005;579(25):5631-4.
157. Dobrovolskaia MA, Neun BW, Clogston JD, Ding H, Ljubimova J, McNeil SE. Ambiguities in applying traditional Limulus Amebocyte Lysate tests to quantify endotoxin in nanoparticle formulations. Nanomedicine. 2010 2010/06/01;5(4):555-62.
158. Cory AH, Owen TC, Barltrop JA, Cory JG. Use of an aqueous soluble tetrazolium/formazan assay for cell growth assays in culture. Cancer Communications. 1991;3(7):207-12.
159. Strober W. Trypan Blue Exclusion Test of Cell Viability. Current Protocols in Immunology. 1997;A.3B:A.3B.1-A.3B.2.
160. Vermes I, Haanen C, Steffens-Nakken H, Reutellingsperger C. A novel assay for apoptosis Flow cytometric detection of phosphatidylserine expression on early apoptotic cells using fluorescein labelled Annexin V. Journal of Immunological Methods. 1995;184(1):39-51.
161. Wilkins RC, Kutzner BC, Truong M, Sanchez-Dardon J, McLean JRN. Analysis of radiation-induced apoptosis in human lymphocytes: Flow cytometry using Annexin V and propidium iodide versus the neutral comet assay. Cytometry. 2002;48(1):14-9.
162. Lacy P, Stow JL. Cytokine release from innate immune cells: association with diverse membrane trafficking pathways. Blood. 2011 July 7, 2011;118(1):9-18.
163. Stow JL, Ching Low P, Offenhäuser C, Sangermani D. Cytokine secretion in macrophages and other cells: Pathways and mediators. Immunobiology. 2009;214(7):601-12.
164. Ng CT, Li JJ, Perumalsamy R, Watt F, Yung LYL, Bay BH. Localizing cellular uptake of nanomaterials in vitro by transmission electron microscopy. Microscopy: Science, Technology, Applications and Education FORMATEX Microscopy Series. 2010;3(4):316-20.
165. Alkilany A, Murphy C. Toxicity and cellular uptake of gold nanoparticles: what we have learned so far? Journal of Nanoparticle Research. 2010;12(7):2313-33.

166. Mayhew TM, Mühlfeld C, Vanhecke D, Ochs M. A review of recent methods for efficiently quantifying immunogold and other nanoparticles using TEM sections through cells, tissues and organs. Annals of Anatomy - Anatomischer Anzeiger. 2009;191(2):153-70.
167. Geiser M, Kreyling WG. Deposition and biokinetics of inhaled nanoparticles. Particle and Fibre Toxicology. 2010;7(2):1-17.
168. Scheffer A, Engelhard C, Sperling M, Buscher W. ICP-MS as a new tool for the determination of gold nanoparticles in bioanalytical applications. Analytical and Bioanalytical Chemistry. 2008;390(1):249-52.
169. Shevchenko A, Tomas H, Havlis J, Olsen JV, Mann M. In-gel digestion for mass spectrometric characterization of proteins and proteomes. Nat Protocols. [10.1038/nprot.2006.468]. 2007;1(6):2856-60.
170. Zhang H, Burnum KE, Luna ML, Petritis BO, Kim J-S, Qian W-J, et al. Quantitative proteomics analysis of adsorbed plasma proteins classifies nanoparticles with different surface properties and size. PROTEOMICS. 2011;11(23):4569-77.
171. Domon B, Aebersold R. Mass Spectrometry and Protein Analysis. Science. 2006 April 14, 2006;312(5771):212-7.
172. Aebersold R, Mann M. Mass spectrometry-based proteomics. Nature. [10.1038/nature01511]. 2003;422(6928):198-207.
173. Ashburner M, Ball CA, Blake JA, Botstein D, Butler H, Cherry JM, et al. Gene Ontology: tool for the unification of biology. Nature Genetics. 2000;25:25 - 9.
174. Kanehisa M, Goto S, Kawashima S, Okuno Y, Hattori M. The KEGG resource for deciphering the genome. Nucleic Acids Research. 2004 January 1, 2004;32(suppl 1):D277-D80.
175. Yih TC, Wei TC. Nanomedicine in cancer treatment. Nanomedicine: Nanotechnology, Biology, and Medicine. 2005;1:191-2.
176. Brinker JC, Sherer GW. Sol – gel science. The physics and chemistry of sol-gel processing. San Diego: Academic Press; 1990.
177. Vigor KL, Kyrtatos PG, Minogue S, Al-Jamal KT, Kogelberg H, Tolner B, et al. Nanoparticles functionalised with recombinant single chain Fv antibody fragments (scFv) for the magnetic resonance imaging of cancer cells. Biomaterials. 2010;31(6):1307-15.
178. Rye PD. Sweet and Sticky: Carbohydrate-Coated Magnetic Beads. Nat Biotech. [10.1038/nbt0296-155]. 1996;14(2):155-7.
179. Tartaj P, del Puerto Morales M, Veintemillas-Verdaguer S, González-Carreño T, Serna CJ. The preparation of magnetic nanoparticles for applications in biomedicine. Journal of Physics D: Applied Physics. 2003;36(13):R182.
180. LaConte L, Nitin N, Bao G. Magnetic nanoparticle probes. Materials Today. 2005;8(5, Supplement 1):32-8.
181. Sosnovik DE, Nahrendorf M, Weissleder R. Magnetic nanoparticles for MR imaging: agents, techniques and cardiovascular applications. Basic research in cardiology. 2008;103(2):122-30.
182. Kunzmann A, Andersson B, Thurnherr T, Krug H, Scheynius A, Fadeel B. Toxicology of engineered nanomaterials: Focus on biocompatibility, biodistribution and biodegradation. Biochimica et Biophysica Acta (BBA) - General Subjects. 2011;1810(3):361-73.
183. Shvedova AA, Kagan VE, Fadeel B. Close Encounters of the Small Kind: Adverse Effects of Man-Made Materials Interfacing with the Nano-Cosmos of Biological Systems. Annual Review of Pharmacology and Toxicology. 2010;50(1):63-88.
184. Gordon S, Taylor PR. Monocyte and macrophage heterogeneity. Nat Rev Immunol. [10.1038/nri1733]. 2005;5(12):953-64.
185. Yu T, Malugin A, Ghandehari H. Impact of Silica Nanoparticle Design on Cellular Toxicity and Hemolytic Activity. ACS Nano. 2011 2011/07/26;5(7):5717-28.
186. Verma A, Stellacci F. Effect of Surface Properties on Nanoparticle–Cell Interactions. Small. 2010;6(1):12-21.
187. Richards D, Ivanisevic A. Inorganic material coatings and their effect on cytotoxicity. Chemical Society Reviews. 2012;41(6).

188. Moghimi SM, Andersen AJ, Hashemi SH, Lettiero B, Ahmadvand D, Hunter AC, et al. Complement activation cascade triggered by PEG–PL engineered nanomedicines and carbon nanotubes: The challenges ahead. Journal of Controlled Release. 2010;146(2):175-81.
189. Rybak-Smith MJ, Sim RB. Complement activation by carbon nanotubes. Advanced Drug Delivery Reviews. 2011;63(12):1031-41.
190. Ehrenberg MS, Friedman AE, Finkelstein JN, Oberdörster G, McGrath JL. The influence of protein adsorption on nanoparticle association with cultured endothelial cells. Biomaterials. 2009;30:603-10.
191. Xia H-B, Yi J, Foo P-S, Liu B. Facile Fabrication of Water-Soluble Magnetic Nanoparticles and Their Spherical Aggregates. Chemistry of Materials. 2007 2007/08/01;19(16):4087-91.